A coherent framework for learning spatiotemporal piecewise- geodesic trajectories from longitudinal manifold-valued data

Juliette Chevallier, Stéphane Oudard, Stéphanie Allassonnière

A Coherent Framework for Learning Spatiotemporal Piecewise-Geodesic Trajectories from Longitudinal Manifold-Valued Data

Juliette Chevallier JULIETTE.CHEVALLIER@POLYTECHNIQUE.EDU
Centre de Mathématiques Appliquées
École polytechnique
Palaiseau, France

Stéphane Oudard STEPHANE.OUDARD@HOP.EGP.AP-HOP-PARIS.FR
Department of Oncology
Hôpital Européen Georges Pompidou
Paris, France

Stéphanie Allassonnière STEPHANIE.ALLASSONNIERE@PARISDESCARTES.FR
Centre de Recherche des Cordeliers
Université Paris Descartes
Paris, France

Editor:

Abstract

This paper provides a coherent framework for studying longitudinal manifold-valued data. We introduce a Bayesian mixed-effects model which allows to estimate both a group-representative piecewise-geodesic trajectory in the Riemannian space of shape and inter-individual variability. We prove the existence of the maximum a posteriori estimate and its asymptotic consistency under reasonable assumptions. Due to the non-linearity of the proposed model, we use a stochastic version of Expectation-Maximization algorithm to estimate the model parameters. Our simulations show that our model is not noise-sensitive and succeed in explaining various paths of progression.

Keywords: Bayesian estimation, EM like algorithm, Longitudinal data, MCMC methods, Nonlinear mixed-effects model, Spatio-temporal analysis

1. Introduction

Longitudinal studies are powerful tools to achieve a better understanding of temporal progressions of biological or natural phenomenons. For instance, longitudinal psychometric data are often used to explore differences in the progression of Alzheimer's and more generally neurodegenerative diseases. Other important applications such as pattern recognition, chemotherapy monitoring, study of face expression dynamics, *etc.* come also from longitudinal studies. Moreover, efforts in medicine and medical follow-up rely more and more on the understanding of a global disease progression and not only on punctual states of health, often with the help of medical images.

Anatomical data – and most of structured data – are naturally modeled as points on a Riemannian manifold, called shape space. Geometrical properties of shape manifolds have

been properly defined over the last decades. Moreover, according to the Whitney embedding theorem (Gallot et al., 2004), as the shape spaces are second-countable, they will always be embedded in a real d-dimensional Euclidean space, the space of measurements, which leads us to consider the shape manifold as a submanifold of this Euclidean space. Therefore, the temporal evolution of empirical data may be modeled as a parametric curve in the space of measurements and more precisely as a noisy version of an underlying parametric curve living on the Riemannian shape submanifold. Given a cohort of individuals followed over a time period, we thus observe discreet samples of such a curve for each subject. We call this set of observations a longitudinal data set.

Mixed-effects models have proved their efficiency in the study of longitudinal data sets (Laird and Ware, 1982), especially for medical purposes (Milliken and Edland, 2000; Ribba et al., 2014). Indeed, mixed-effects models provide a general and flexible framework to study correlated data. They consist of two parts: fixed effects which describe the data at the population level and random effects which are associated with individual experimental units drawn at random from a population. Given a longitudinal data set, our model aims at estimating a representative trajectory of the whole population progression and its variability. Then, we can define subject-specific trajectories in view of the global progression.

The recent generic approach of Schiratti et al. (2015, 2017) to align patients is even more suitable. This model was built with the aim of granting temporal and spatial inter-subject variability through individual variations of a common time-line grant and parallel shifting of a representative trajectory. Each individual trajectory has its own intrinsic geometric pattern through spacial variability and its own time parametrization through time variability. In term of modeling, the time variability allows some individuals to follow the same progression path but at a different age and with possibly a different pace. However, Schiratti et al. (2015, 2017) have made a strong hypothesis to build their model as they assume the characteristic evolution to be geodesic. Such an assumption significantly reduces the effective framework of their model. In this paper, we will relax this assumption to make the model applicable to a wider variety of situations and data sets: we address each situation in which the evolution can fluctuate several times.

We propose in this paper a coherent and generic statistical framework which includes the model of Schiratti et al. (2015, 2017). Following their approach, we define a nonlinear mixed-effects model for the definition and estimation of spatio-temporal piecewise-geodesic trajectories from longitudinal manifold-valued data. We estimate a representative piecewise-geodesic trajectory of the global progression and together with spacial and temporal inter-individual variabilities. Particular attention is paid to estimation of the correlation between the different phases of the evolution.

Estimation is formulated as a well-defined *maximum a posteriori* (MAP) problem which we prove to be consistent under mild considerations. Numerically, the MAP estimation of the parameters is performed through a stochastic version of the the expectation-maximization (EM) algorithm (Dempster et al., 1977), namely the Markov chain Monte Carlo stochastic-approximation expectation-maximization (MCMC-SAEM) algorithm (Lavielle, 2014). Theoretical results regarding its convergence have been proved in Delyon et al. (1999) and Allassonnière et al. (2010) and its numerical efficiency has been demonstrated for these types of models (Schiratti et al. (2015, 2017), Monolix – `http://lixoft.com/`).

The paper is organized as follows: in Section 2 we define a generic nonlinear mixed-effects model for piecewise-geodesically distributed data. Riemannian geometry allows us to derive a method that makes light assumptions about the data and applications we are able to deal with. We then make the generic formulation explicit for one-dimension manifolds and piecewise-logistically distributed data in Section 4. This particular case is built in the target of chemotherapy monitoring. In Section 3, we explain how to use the MCMC-SAEM algorithm to produce MAP estimates of the parameters. We also prove a consistency theorem, whose proof is postponed in appendix A. In Section 5, some experiments are performed for the piecewise-logistic model: both on synthetic and on real data from the Hôpital Européen Georges Pompidou (HEGP). These experiments highlight the robustness of our model to noise and its performance in understanding individual paths of progression.

2. Generic Mixed-Effects Model for Piecewise-Geodesically Distributed Data on a Riemannian Manifold

In the following, we describe a *generic* method to build mixed-effects models for piecewise-geodesically distributed data. This leads us to a large variety of possible situations that we will be able to deal with within the same framework. This model has been first introduced in Chevallier et al. (2017).

We consider a longitudinal data set $\boldsymbol{y}$ obtained by repeating multivariate measurements of $n \in \mathbb{N}^*$ individuals, where each individual $i \in [\![1, n]\!]$ is observed $k_i \in \mathbb{N}^*$ times, at the time points $\boldsymbol{t}_i = (t_{i,j})_{j \in [\![1,k_i]\!]}$ and where $\boldsymbol{y}_i = (y_{i,j})_{j \in [\![1,k_i]\!]}$ denotes the sequence of observations for this individual. We also denote $k = \sum_{i=1}^{n} k_i$ the total numbers of observations and assume that each observation $y_{i,j}$ is a point of $\mathbb{R}^d$ where $d \in \mathbb{N}$. Thus, the observed data consist in a sequence $\boldsymbol{y} = (y_{i,j})_{(i,j) \in [\![1,n]\!] \times [\![1,k_i]\!]}$ of $\mathbb{R}^{kd}$, where $[\![1, n]\!] \times [\![1, k_i]\!]$ denotes for compactness the set $\{(i, j) | i \in [\![1, n]\!] \wedge j \in [\![1, k_i]\!]\}$.

We generalize the idea of Schiratti et al. (2015, 2017) and build our model in a hierarchical way. Our data points are seen as noisy samples along trajectories and we suppose that each individual trajectory derives from a group-representative scenario through spatiotemporal transformations. Key to our model is that the group-representative trajectory in no longer assumed to be geodesic but piecewise-geodesic.

To ensure that the optimization of those trajectories can be computationally performed in a reasonable amount of time, we build a parametric model. That is to say that the trajectories depend on a finite number of variables. In the following (see Subsection 2.3), we will denote $\boldsymbol{z}_{\text{pop}}$ the variables driving the group-representative scenario and $\boldsymbol{z}_i$ those associated to the individual $i \in [\![1, n]\!]$. For the sake of clarity, we first detail the construction of the trajectories from a geometrical point of view. Then, we state our generative model in a statistical perspective.

2.1 The Group-Representative Trajectory

Let $m \in \mathbb{N}^*$ and $\boldsymbol{t_R} = \left(-\infty < t_R^1 < \ldots < t_R^{m-1} < +\infty\right)$ a subdivision of $\mathbb{R}$, called the *breaking-up times* sequence. In order the representative trajectory γ_0 to be geodesic on each of the m sub-intervals of $\boldsymbol{t_R}$, we build γ_0 component by component.

2.1.1 A Piecewise-Geodesic Curve

In this context, let M_0 be a geodesically complete submanifold of $\mathbb{R}^d$, $\left(\bar{\gamma}_0^\ell\right)_{\ell\in[\![1,m]\!]}$ a family of geodesics on M_0 and $\left(\phi_0^\ell\right)_{\ell\in[\![1,m]\!]}$ a family of isometries defined on M_0. For all $\ell \in [\![1, m]\!]$, we set $M_0^\ell = \phi_0^\ell(M_0)$ and $\gamma_0^\ell = \phi_0^\ell \circ \bar{\gamma_0}^\ell$. The isometric nature of the mapping ϕ_0^ℓ ensures that the manifolds M_0^ℓ remain Riemannian and that the curves $\gamma_0^\ell \colon \mathbb{R} \to M_0^\ell$ remain geodesic. In particular, each γ_0^ℓ remains parametrizable (Gallot et al., 2004). We define the representative trajectory γ_0 by

$$\forall t \in \mathbb{R}, \quad \gamma_0(t) \;=\; \gamma_0^1(t)\,\mathbb{1}_{]-\infty,t_R^1]}(t) \;+\; \sum_{\ell=2}^{m-1} \gamma_0^\ell(t)\,\mathbb{1}_{]t_R^{\ell-1},t_R^\ell]}(t) \;+\; \gamma_0^m(t)\,\mathbb{1}_{]t_R^{m-1},+\infty[}(t)\,.$$

In other words, given a *manifold-template* of the geodesic components M_0, we build γ_0 so that the restriction of γ_0 to each sub-interval of $\boldsymbol{t_R}$ is the deformation of a geodesic curve $\bar{\gamma}_0^\ell$ living on M_0 by the corresponding isometry ϕ_0^ℓ. In practice, M_0 is chosen in order to catch the geometric nature of the observed data : if we are studying a score as in Section 4, M_0 will be the standard finite segment $]0, 1[$ for instance. The choice of the isometries ϕ_0^ℓ and the geodesics $\bar{\gamma}_0^\ell$ have to be done with the aim of having an "as regular as possible" (at least continuous) curve γ_0 at the breaking-up time points t_R^ℓ. In the following section, we propose a way to meet this criterion in one dimension. Moreover, the freedoms in the choice of ϕ_0^ℓ and $\bar{\gamma}_0^\ell$ induce a wide panel of models.

2.1.2 Boundary Conditions

Because of the piecewise nature of our representative trajectory γ_0, constraints have to be formulated on each interval of the subdivision $\boldsymbol{t_R}$. Following the formulation of the *local existence and uniqueness theorem* (Gallot et al., 2004), constraints on geodesics are generally formulated by forcing a value and a tangent vector at a given time-point. However, as soon as there is more that one geodesic component, *i.e.* $m > 1$, such an approach cannot ensure the curve γ_0 to be at least continuous. That is why we re-formulate these constraints in our model as boundary conditions. Let $\bar{\boldsymbol{A}} = (\bar{A}^0, \ldots, \bar{A}^m) \in (M_0)^{m+1}$. Let $t_0 \in \mathbb{R}$ be a real value representing an initial time and $t_1 \in \mathbb{R}$ representing a final one. We impose that for all $\ell \in [\![1, m-1]\!]$,

$$\bar{\gamma}_0^1(t_0) = \bar{A}^0\ , \quad \bar{\gamma}_0^\ell(t_R^\ell) = \bar{A}^\ell\ , \quad \bar{\gamma}_0^{\ell+1}(t_R^\ell) = \bar{A}^\ell \quad \text{and} \quad \bar{\gamma}_0^m(t_1) = \bar{A}^m\,.$$

Notably, the $2m$ constraints are defined step by step. In the case where the geodesics could be written explicitly, such constraints do not complicate the model. In more complicated case, we use shooting or matching methods to enforce this constraints.

From this representative curve, we derive a modeling of the individual trajectories that mimics the individual evolution of subjects and best fits the individual observations.

2.2 Individual Trajectories: Space and Time Warping

We want the individual trajectories to represent a wide variety of behaviors and to derive from the group characteristic path by spatiotemporal transformations. To do that, we define for each component of the piecewise-geodesic curve γ_0 a couple of transformations: the

diffeomorphic component deformations and the *time component reparametrizations* which characterize respectively the spatial and the temporal variability of propagation among the population. Moreover, we decree as few constraints as possible in the construction: at least continuity and control of the slopes at the (individual) breaking-up points.

2.2.1 Time Component Reparametrizations

For compactness, we denote t_0 by t_R^0 from now on.

To allow different paces in the progression and different rupture times for each individual, we introduce some temporal transformations $\psi_i^\ell \colon \mathbb{R} \to \mathbb{R}$, called *time-warp*, that are defined for the subject $i \in [\![1, n]\!]$ and for the geodesic component $\ell \in [\![1, m]\!]$ by

$$\psi_i^\ell(t) = \psi_{i\,(\alpha_i^\ell, \tau_i^\ell)}^\ell(t) = \alpha_i^\ell(t - t_R^{\ell-1} - \tau_i^\ell) + t_R^{\ell-1} \quad \text{where} \quad (\alpha_i^\ell, \tau_i^\ell) \in \mathbb{R}^+ \times \mathbb{R}\,.$$

The parameters τ_i^ℓ correspond to the time-shifts between the representative and the individual progression onset ; the α_i^ℓ are the acceleration factors that describe the pace of individuals, being faster or slower than the population characteristic. For all individual $i \in [\![1, n]\!]$, let $\boldsymbol{t_R}_{,i} = (t_{R,i}^\ell)_{\ell \in [\![1, m-1]\!]}$ denote the individual sequence of rupture times which is the subdivision of $\mathbb{R}$ such that for all $\ell \in [\![1, m-1]\!]$, $\psi_i^\ell(t_{R,i}^\ell) = t_R^\ell$ *i.e.* such that

$$t_{R,i}^\ell = t_{R,i\,(\alpha_i^\ell, \tau_i^\ell)}^\ell = t_R^{\ell-1} + \tau_i^\ell + \frac{t_R^\ell - t_R^{\ell-1}}{\alpha_i^\ell}\,.$$

To ensure good adjunction at the rupture times, we demand that for all $\ell \in [\![1, m]\!]$, $\psi_i^\ell(t_{R,i}^{\ell-1}) = t_R^{\ell-1}$. Hence the time reparametrizations are constrained and only the acceleration factors α_i^ℓ and the first time shift τ_i^1 are free: all other time shift, $\ell \in [\![2, m]\!]$, are defined by $\tau_i^\ell = t_{R,i}^{\ell-1} - t_R^{\ell-1}$.

In the following, we will sometimes refer to the individual initial and final times which are defined, for all $i \in [\![1, n]\!]$, by $t_0^i = t_0 + \tau_1$ and $t_1^i = t_R^{m-1} + \tau_i^m + \frac{t_1 - t_R^{m-1}}{\alpha_i^m}$.

2.2.2 Diffeomorphic Component Deformations

Concerning the space variability, we introduce m diffeomorphisms $\phi_i^\ell \colon M_0^\ell \to \phi_i^\ell(M_0^\ell)$ to enable the different components of the individual trajectories to vary more irrespectively of each other. We just enforce the adjunctions to be at least continuous and therefore the mappings ϕ_i^ℓ to satisfy $\phi_i^\ell \circ \gamma_0^\ell(t_R^\ell) = \phi_i^{\ell+1} \circ \gamma_0^{\ell+1}(t_R^\ell)$ for all $\ell \in [\![1, m-1]\!]$. Note that, as the individual paths are no longer required to be geodesic, the mappings ϕ_i^ℓ do not need to be isometric.

For all individual $i \in [\![1, n]\!]$ and all component $\ell \in [\![1, m]\!]$, we set $\gamma_i^\ell = \phi_i^\ell \circ \gamma_0^\ell \circ \psi_i^\ell$ and define the corresponding individual curve γ_i by

$$\forall t \in \mathbb{R}, \quad \gamma_i(t) \;=\; \gamma_i^1(t)\, \mathbb{1}_{]-\infty, t_{R,i}^1]}(t) \;+\; \sum_{\ell=2}^{m-1} \gamma_i^\ell(t)\, \mathbb{1}_{]t_{R,i}^{\ell-1}, t_{R,i}^\ell]}(t) \;+\; \gamma_i^m(t)\, \mathbb{1}_{]t_{R,i}^{m-1}, +\infty[}(t)\,.$$

Finally, the observations $\boldsymbol{y}_i = (y_{i,j})_{j \in [\![1, k_i]\!]}$ are assumed to be distributed along the curve γ_i and perturbed by an additive Gaussian noise $\boldsymbol{\varepsilon}_i \sim \mathcal{N}(0, \sigma^2 I_{k_i d})$ where $\sigma \in \mathbb{R}^+$:

$$\forall (i, j) \in [\![1, n]\!] \times [\![1, k_i]\!], \quad y_{i,j} \;=\; \gamma_i(t_{i,j}) \;+\; \varepsilon_{i,j} \quad \text{where} \quad \varepsilon_{i,j} \sim \mathcal{N}(0, \sigma^2 I_d)\,.$$

By construction, for each $(i,j) \in [\![1,n]\!] \times [\![1,k_i]\!]$, there exist $\ell \in [\![1,m]\!]$ such that $\gamma_i(t_{i,j})$ lies on the submanifold $\phi_i^\ell(M_0^\ell)$ of $\mathbb{R}^d$. Thus, the previous sum is well-defined. In particular, we do not assume that the noisy-observation remain on the manifold.

The choice of the isometries ϕ_0^ℓ and the diffeomorphisms ϕ_i^ℓ induces a large range of piecewise-geodesic models. For example, if $m = 1$, $\phi_0^1 = Id$ and if ϕ_i^1 denotes the application that maps a curve onto its parallel curve for a given non-zero tangent vector $\boldsymbol{w}_i$, we feature the model proposed by Schiratti et al. (2015, 2017). In Section 4.1, we propose another specific model which can be used for chemotherapy monitoring for instance.

2.3 Toward a Coherent and Tractable Statistical Generative Model

We first introduce some notations in order to clearly state our statistical generative model. Let $\boldsymbol{z}_i^\psi = (\alpha_i^\ell, \tau_i^\ell)_{\ell \in [\![1,m]\!]}$ denote the individual temporal variables and similarly $\boldsymbol{z}_i^\phi$ denote the individual spatial variables, *i.e.* the variables associated to the variation of the m diffeomorphic deformations ϕ_i^ℓ. Likewise, let $\boldsymbol{z}_{\text{pop}}$ denote the population variable, *i.e.* the variable associated to the variation of the m isometric mappings ϕ_0^ℓ.

Let $p_{\text{ind}} \in \mathbb{N}$ be the dimension of each vector $\boldsymbol{z}_i = (\boldsymbol{z}_i^\psi, \boldsymbol{z}_i^\phi)$ such that $\forall i \in [\![1,n]\!]$, $\mathcal{Z}_i \subset \mathbb{R}^{p_{\text{ind}}}$ denotes the space of random effects. Similarly, let $p_{\text{pop}} \in \mathbb{N}$ be the dimension of $\boldsymbol{z}_{\text{pop}}$ and $\mathcal{Z}_{\text{pop}} \subset \mathbb{R}^{p_{\text{pop}}}$ denotes the space of fixed effects.

To cover many situations, we do not explicit here the individual spatial variables $\boldsymbol{z}_i^\phi$. However, for examples, we propose an instantiation of this generic model for one-dimension manifolds and piecewise-logistically distributed data at Section 4. Moreover, our generic approach encompass a large variety of models as such proposed by Schiratti et al. (2017), Bône et al. (2018) and Koval et al. (2018).

2.3.1 Modeling Constraints...

In a modeling perspective, we are interested in understanding the individual behaviors with respect to the characteristic one. Thus, we focus on the variance of the random effects $\boldsymbol{z}_i = (\boldsymbol{z}_i^\psi, \boldsymbol{z}_i^\phi)$ rather than their marginal distributions. Moreover, as we want the representative path to characterize the pattern of behavior of the individual trajectories, we have to slightly modify the individual parameters $\boldsymbol{z}_i$ in such a way that for all i, $\mathbb{E}(\boldsymbol{z}_i) = 0$. In particular, if our model were linear, this would have ensure the representative trajectory to be the mean (in the statistical meaning) of the individual ones. Concerning the individual temporal variables for instance, the acceleration parameters $(\alpha_i^\ell)_{\ell \in [\![1,m]\!]}$ have to be positive and equal to one on average while the time shifts $(\tau_i^\ell)_{\ell \in [\![1,m]\!]}$ are of any signs and must be zero on average. For these reasons, we set $\alpha_i^\ell = \mathrm{e}^{\xi_i^\ell}$ and consider the "new" temporal variable, still denoted $\boldsymbol{z}_i^\psi$ for compactness, $\boldsymbol{z}_i^\psi = (\xi_i^\ell, \tau_i^\ell)_{\ell \in [\![1,m]\!]}$. We proceed in the same way for the individual spatial variables z_i^ϕ, when required (for centered or positive variables).

To sum up, we assume that there exists a symmetric positive-definite matrix $\Sigma \in \mathscr{S}_{p_{\text{ind}}}^+(\mathbb{R})$ such that $\boldsymbol{z}_i \sim \mathcal{N}(0, \Sigma)$, and now want to estimate Σ. Hence, the parameters we are interested in are $\theta = (\boldsymbol{z}_{\text{pop}}, \Sigma, \sigma) \in \mathcal{Z}_{\text{pop}} \times \mathscr{S}_{p_{\text{ind}}}^+(\mathbb{R}) \times \mathbb{R}^+$.

2.3.2 ...and Computational Feasibility

Given a n-sample, we target $\hat{\theta}_n$ an estimation of our parameters. Following the classical approach for maximum likelihood estimation in nonlinear mixed-effects models, we use the MCMC-SAEM algorithm. However, the theoretical convergence of this algorithm is proved only if the model belongs to the curved exponential family (Delyon et al., 1999; Allassonnière et al., 2010). This framework is also important for numerical performances. Without further hypothesis, our model does not satisfy this constraint. Therefore, we proceed as in Kuhn and Lavielle (2005): we assume that $\boldsymbol{z}_{\text{pop}}$ is the realization of independent Gaussian random variables with fixed small variances and estimate the means of those variables. So, the parameters we want to estimate are $\theta = (\overline{\boldsymbol{z}_{\text{pop}}}, \Sigma, \sigma)$ and we define the set of admissible parameters by $\Theta = \mathbb{R}^{p_{\text{pop}}} \times \mathscr{S}^+_{p_{\text{ind}}}(\mathbb{R}) \times \mathbb{R}^+$.

The fixed and random effects $\boldsymbol{z} = (\boldsymbol{z}_{\text{pop}}, \boldsymbol{z}_i)_{i \in [\![1,n]\!]}$ are considered as latent variables. Our model writes in a hierarchical way as

$$\boldsymbol{y} \,|\, \boldsymbol{z}, \theta \sim \bigotimes_{i=1}^{n} \bigotimes_{j=1}^{k_i} \mathscr{N}\left(\gamma_i(t_{i,j}), \sigma^2\right) \quad \text{and} \quad \boldsymbol{z} \,|\, \theta \sim \mathscr{N}\left(\overline{\boldsymbol{z}_{\text{pop}}}, \mathcal{D}_{\text{pop}}^{-1}\right) \bigotimes_{i=1}^{n} \mathscr{N}(0, \Sigma)$$

where $\boldsymbol{\sigma}_{\text{pop}} \in \mathbb{R}_+^{p_{\text{pop}}}$ is an hyperparameter of the model and $\mathcal{D}_{\text{pop}} = \boldsymbol{\sigma}_{\text{pop}}^2 I_{p_{\text{pop}}} \in \mathscr{M}_{p_{\text{pop}}}(\mathbb{R})$. The products $\otimes$ mean that the corresponding entries are considered to be independent. In other words, we assume that each of the measurement noises is independent of all the others. Of course, it may not be the case in practice. But, as all the observations for a given subject come from a single curve, this assumption is reasonable in our context. Moreover, this assumption leads us to a more computationally tractable algorithm.

3. Parameters Estimation

As said just above, we want to estimate $\theta = (\overline{\boldsymbol{z}_{\text{pop}}}, \Sigma, \sigma) \in \mathbb{R}^{p_{\text{pop}}} \times \mathscr{S}^+_{p_{\text{ind}}}(\mathbb{R}) \times \mathbb{R}^+$. As we want our model to be consistent with high-dimensional data analysis, we consider a Bayesian framework, *i.e.* we assume the following priors

$$(\Sigma, \sigma) \sim \mathcal{W}^{-1}(V, m_\Sigma) \otimes \mathcal{W}^{-1}(v, m_\sigma) \quad \text{where} \quad V \in \mathscr{S}^+_{p_{\text{ind}}}(\mathbb{R}), \quad v, m_\Sigma, m_\sigma \in \mathbb{R}$$

and $\mathcal{W}^{-1}(V, m_\Sigma)$ denotes the inverse Wishart distribution with scale matrix V and degrees of freedom m_Σ. Regularization has indeed proven its fruitful in this context (Giraud, 2014). In order for the inverse Wishart to be non-degenerate, the degrees m_Σ and m_σ must satisfy $m_\Sigma > 2p_{\text{ind}}$ and $m_\sigma > 2$. In practice, we yet use degenerate priors but with well-defined posteriors. In the spirit of the one-dimension inverse Wishart distribution, we define the density function distribution of higher dimension as

$$f_{\mathcal{W}^{-1}(V, m_\Sigma)}(\Sigma) = \frac{1}{\Gamma_{p_{\text{ind}}}\left(\frac{m_\Sigma}{2}\right)} \left(\frac{\sqrt{|V|}}{2^{\frac{p_{\text{ind}}}{2}} \sqrt{|\Sigma|}} \exp\left(-\frac{1}{2} \operatorname{tr}\left(V \Sigma^{-1}\right) \right) \right)^{m_\Sigma}$$

where $\Gamma_{p_{\text{ind}}}$ is the multivariate gamma function and, for all matrices A, $|A|$ denotes the determinant of the matrix A.

The estimates are obtained by maximizing the posterior density on θ conditionally on the observations $\boldsymbol{y} = (y_{i,j})_{(i,j)\in[\![1,n]\!]\times[\![1,k_i]\!]}$.

In the following paragraphs, we first show that the model is well-posed *i.e.* that for any finite sample the *maximum* we are looking for exists. We then prove a consistency theorem which ensures that the set of parameters which well-explain the observations is non-empty and that the MAP estimator converges to this set. Last, we explain how to use the MCMC-SAEM algorithm to produce MAP estimates.

3.1 Existence of the Maximum a Posteriori Estimator

The inverse Wishart priors on the variances not only regularize the log-likelihood of the model, they also ensure the existence of the MAP estimator.

Theorem 1 (Existence of the MAP estimator) *Given a piecewise-geodesic model and the choice of probability distributions for the parameters and latent variables of the model, for any data set $(t_{i,j}, y_{i,j})_{(i,j)\in[\![1,n]\!]\times[\![1,k_i]\!]}$, there exists $\widehat{\theta}_{\mathrm{MAP}} \in \underset{\theta\in\Theta}{\mathrm{argmax}}\, q\big(\theta|\boldsymbol{y}\big)$.*

The demonstration of the theorem uses the following lemma.

Lemma 1 *Given a piecewise-geodesic model and the choice of a probability distribution for the parameters and latent variables of the model, the posterior $\theta \mapsto q\big(\theta|\boldsymbol{y}\big)$ is continuous on the parameter space Θ.*

Proof Let $\mathcal{Z} = \mathcal{Z}_{\mathrm{pop}} \times \prod_{i=1}^{n} \mathcal{Z}_i$ denote the space of latent variables. Using Bayes rule, for all $\theta \in \Theta$,

$$q\big(\,\theta\,|\,\boldsymbol{y}\,\big) = \frac{1}{q(\boldsymbol{y})} \left(\int_{\mathcal{Z}} q\big(\,\boldsymbol{y}\,|\,\boldsymbol{z},\theta\,\big)\; q\big(\,\boldsymbol{z}\,|\,\theta\,\big)\,\mathrm{d}\boldsymbol{z} \right) q_{prior}(\theta)\,.$$

The density functions $\theta \mapsto q_{prior}(\theta)$ and $\theta \mapsto q\big(\boldsymbol{y}|\boldsymbol{z},\theta\big)\, q\big(\boldsymbol{z}|\theta\big)$ are continuous on Θ for all $\boldsymbol{z} \in \mathcal{Z}$. Moreover, for all $\theta \in \Theta$ and all $\boldsymbol{z} \in \mathcal{Z}$,

$$q\big(\,\boldsymbol{y}\,|\,z,\theta\,\big) = \frac{1}{(\sigma\sqrt{2\pi})^k} \exp\left(-\frac{1}{2\sigma^2} \sum_{i=1}^{n} \sum_{j=1}^{k_i} \big(y_{i,j} - \gamma_i(t_{i,j})\big)^2 \right)$$

and so, for all $\theta \in \Theta$ and $\boldsymbol{z} \in \mathcal{Z}$, $q\big(\boldsymbol{y}|\boldsymbol{z},\theta\big)\, q\big(\boldsymbol{z}|\theta\big) \leqslant \frac{1}{(\sigma\sqrt{2\pi})^k}\, q\big(\boldsymbol{z}|\theta\big)$ which is positive and integrable as a probability distribution. As a consequence, $\boldsymbol{z} \mapsto q\big(\boldsymbol{y}|\boldsymbol{z},\theta\big)\, q\big(\boldsymbol{z}|\theta\big)$ is integrable – and positive – on $\mathcal{Z}$ for all $\theta \in \Theta$ and $\theta \mapsto q\big(\boldsymbol{y}|\theta\big)$ is continuous. ■

Proof [Theorem 1 – Existence of the MAP] We use the Alexandrov one-point compactification $\overline{\Theta} = \Theta \cup \{\infty\}$ of the parameters space Θ, where a sequence $(\theta_n)_{n\in\mathbb{N}}$ converges toward the point ∞ if and only if it eventually steps out of every compact subset of Θ. Thus, given the result of Lemma 1, it suffices to prove that $\lim_{\theta\to\infty} \log\, q\big(\theta|\boldsymbol{y}\big) = -\infty$. We keep the notation of the previous proof and proceed similarly. In particular, for all $\theta \in \Theta$,

$$\log\, q\big(\theta|\boldsymbol{y}\big) \;\leqslant\; -\log\, q(\boldsymbol{y}) - k\log(\sqrt{2\pi}) - k\log(\sigma) + \log\, q_{prior}(\theta)\,.$$

By computing the prior distribution q_{prior}, we remark that there exists λ which does not depend on the parameter θ such as

$$\log q\big(\theta|\boldsymbol{y}\big) \;\leqslant\; \lambda(\boldsymbol{y}) - (k+m_\sigma)\log(\sigma) - \frac{m_\Sigma}{2}\log(|\Sigma|) - \frac{m_\Sigma}{2}\operatorname{tr}\left(V\Sigma^{-1}\right) - \frac{m_\sigma}{2}\left(\frac{v}{\sigma}\right)^2 .$$

Let $\mu(V)$ denote the smallest eigenvalue of V, $\rho(\Sigma^{-1})$ the largest eigenvalue of Σ^{-1}, which is also its operator norm, and $\left\langle\, \Sigma \;\middle|\; V \,\right\rangle_F$ the Frobenius inner product of Σ with V. We know that $\left\langle\, \Sigma \;\middle|\; V \,\right\rangle_F \geqslant \mu(V)\,\rho(\Sigma^{-1})$ and $\log(|\Sigma^{-1}|) \leqslant p_{\text{ind}}\,\log\big(\,\|\Sigma^{-1}\|\,\big)$ so that

$$-\frac{m_\Sigma}{2}\operatorname{tr}\left(V\Sigma^{-1}\right) + \frac{m_\Sigma}{2}\log(|\Sigma^{-1}|) \;\leqslant\; \frac{m_\Sigma}{2}\left[\,-\mu(V)\,\|\Sigma^{-1}\| \;+\; p_{\text{ind}}\,\log\big(\,\|\Sigma^{-1}\|\,\big)\,\right] \qquad (1)$$

and

$$\lim_{\|\Sigma\|+\|\Sigma^{-1}\|\to+\infty} \left\{\; -\frac{m_\Sigma}{2}\operatorname{tr}\left(V\Sigma^{-1}\right) + \frac{m_\Sigma}{2}\log(|\Sigma^{-1}|) \;\right\} = -\infty\,.$$

Likewise,

$$\lim_{\sigma+\sigma^{-1}\to+\infty} \left\{\; -(k+m_\sigma)\log(\sigma) - \frac{m_\sigma}{2}\left(\frac{v}{\sigma}\right)^2 \;\right\} = -\infty$$

hence the result. ■

We have detailed the previous proof in order to emphasize the necessity of prior distribution on the variances Σ and σ to ensure the existence of the *maximum a posteriori*.

3.2 Consistency of the Maximum a Posteriori Estimator

We are interested in the consistency of the MAP estimator without making strong assumptions on the distribution of the observations $\boldsymbol{y}$. In particular, we do not assume that the observations are generated by the model.

We denote $P(\mathrm{d}\boldsymbol{y})$ the distribution governing the observations and Θ_* the set of admissible parameters inducing a model distribution close to $P(\mathrm{d}\boldsymbol{y})$:

$$\Theta_* = \left\{ \theta_* \in \Theta \;\middle|\; \mathbb{E}_{P(\mathrm{d}\boldsymbol{y})}\left[\log q(\boldsymbol{y}|\theta_*)\right] = \sup_{\theta\in\Theta^\omega} \mathbb{E}_{P(\mathrm{d}\boldsymbol{y})}\left[\log q(\boldsymbol{y}|\theta)\right] \right\} .$$

The MAP estimator is said consistent if it converges to the set Θ_* (on every compact of Θ possibly). Classical results of consistency assume that the space Θ_* is non-empty (see the Wald's consistency theorem (van der Vaart, 2000)). However, such an hypothesis is not entirely satisfactory: we have no guarantee that Θ_* is actually non-empty. We propose below a reasonable framework in which the convergence of the MAP estimator toward the corresponding non-empty set Θ_* is guaranteed.

3.2.1 Two Kinds of Latent Variables

To this end and for any $\omega \in \mathbb{R}^+$, we define the space Θ^ω of admissible parameters such that on average, the fixed effects are bounded by ω:

$$\Theta^\omega = \{\theta = (\overline{\boldsymbol{z}_{\text{pop}}}, \Sigma, \sigma) \in \Theta \mid \|\overline{\boldsymbol{z}_{\text{pop}}}\|_2 \leqslant \omega\} \quad \text{where} \quad \Theta = \mathbb{R}^{p_{\text{pop}}} \times \mathscr{S}^+_{p_{\text{ind}}}(\mathbb{R}) \times \mathbb{R}^+ .$$

As the assumption only concern the average behavior of the population variable $\boldsymbol{z}_{\text{pop}}$, it is not restrictive. Moreover, fixed effects are most of the time bounded (but potentially with high bounds) in applications. In this new framework, for all $\omega \in \mathbb{R}^+$,

$$\Theta_*^\omega = \left\{\theta \in \Theta^\omega \;\middle|\; \mathbb{E}_{P(\mathrm{d}\boldsymbol{y})}\left[\log q(\boldsymbol{y}|\theta)\right] = \mathbb{E}^*(\omega)\right\} \quad \text{where} \quad \mathbb{E}^*(\omega) = \sup_{\theta\in\Theta^\omega} \mathbb{E}_{P(\mathrm{d}\boldsymbol{y})}\left[\log q(\boldsymbol{y}|\theta)\right].$$

To state the consistency of the MAP estimator, we first have to give some notations. For all $i \in [\![1,n]\!]$, we assume the existence of two subsets of $\mathcal{Z}_i$ – $\mathcal{Z}_i^{\text{reg}}$ and $\mathcal{Z}_i^{\text{crit}}$ – such that $\mathcal{Z}_i = \mathcal{Z}_i^{\text{reg}} \times \mathcal{Z}_i^{\text{crit}}$. In other words, we assume that each component of each individual latent variable $\boldsymbol{z}_i$ is of two sorts: *regular* or *critical*. We will respectively denote $\boldsymbol{z}_i^{\text{reg}}$ and $\boldsymbol{z}_i^{\text{crit}}$ this sub-variables leading to write, up to permutations, $\boldsymbol{z}_i = (\boldsymbol{z}_i^{\text{reg}}, \boldsymbol{z}_i^{\text{crit}})$. Likewise, we assume that the components of the population latent variables can be regular or critical, *i.e.* that there exists $\mathcal{Z}_{\text{pop}}^{\text{reg}}, \mathcal{Z}_{\text{pop}}^{\text{crit}} \subset \mathcal{Z}_{\text{pop}}$ such that $\boldsymbol{z}_{\text{pop}} = (\boldsymbol{z}_{\text{pop}}^{\text{reg}}, \boldsymbol{z}_{\text{pop}}^{\text{crit}}) \in \mathcal{Z}_{\text{pop}}^{\text{reg}} \times \mathcal{Z}_{\text{pop}}^{\text{crit}}$. To stay consistent with the previous notations, we denote $p_{\text{ind}}^{\text{reg}}$, $p_{\text{ind}}^{\text{crit}}$, $p_{\text{pop}}^{\text{reg}}$ and $p_{\text{pop}}^{\text{crit}}$ the dimension of the ambient space of the matching sets: $\mathcal{Z}_i^{\text{reg}} \subset \mathbb{R}^{p_{\text{ind}}^{\text{reg}}}$ and so on.

3.2.2 Consistency of the Maximum a Posteriori Estimator

In the following, we want to study the effect of the variables $(\boldsymbol{z}_{\text{pop}}, \boldsymbol{z}_i)$ on the trajectories. To this end, we introduce for all i the notation $\vec{\boldsymbol{\gamma}}_i(\boldsymbol{z}_{\text{pop}}, \boldsymbol{z}_i) = (\gamma_i(t_{i,j}))_{j\in[\![1,k_i]\!]} \in \mathbb{R}^{k_i}$ and more generally the functions $\vec{\boldsymbol{\gamma}}_i \colon \mathcal{Z}_{\text{pop}} \times \mathcal{Z}_i \to \mathbb{R}^{k_i}$. Let $\ell \in [\![1,n]\!]$, consider a ℓ-tuple of individuals and denote by $k^\ell = \sum_{i=1}^{\ell} k_i$ the total number of measures for this ℓ-tuple. Let $\boldsymbol{y}^\ell = (y_i)_{i\in[\![1,\ell]\!]} \in \mathbb{R}^{k^\ell}$ and $\boldsymbol{z}^\ell = (\boldsymbol{z}_{\text{pop}}, \boldsymbol{z}_i)_{i\in[\![1,\ell]\!]} \in \mathbb{R}^{p_{\text{pop}}+\ell\, p_{\text{ind}}}$ be the vectors made up of the ℓ corresponding vectors. As in the one-by-one case, we define by $\vec{\boldsymbol{\gamma}}^\ell \colon \mathcal{Z}_{\text{pop}} \times \mathcal{Z}_i^\ell \to \mathbb{R}^{k^\ell}$ the function which maps the vector $\boldsymbol{z}^\ell$ to the one $(\vec{\boldsymbol{\gamma}}_i(\boldsymbol{z}_{\text{pop}}, \boldsymbol{z}_i))_{i\in[\![1,\ell]\!]}$.

For all vectors of the form $(\boldsymbol{a}, \boldsymbol{b}) \in \mathbb{R}^{p_a} \times \mathbb{R}^{p_b}$ where p_a and p_b are any integer number and for all indices $v \in [\![1, p_a + p_b]\!]$, $(\boldsymbol{a}, \boldsymbol{b})_v$ and $(\boldsymbol{a}, \boldsymbol{b})_{-v}$ refer respectively to

$$(\boldsymbol{a}, \boldsymbol{b})_v = \big(\,(a_1, \dots, a_{p_a})\,,\,(b_1, \dots, b_{p_b})\,\big)_v = \begin{cases} a_v & \text{if } \; v \leqslant p_a \\ b_{v-p_a} & \text{else} \end{cases}$$

$$(\boldsymbol{a}, \boldsymbol{b})_{-v} = \begin{cases} \big(\,(a_1, \dots, a_{v-1}, a_{v+1}, \dots, a_{p_a})\,,\,(b_1, \dots, b_{p_b})\,\big) & \text{if } \; v \leqslant p_a \\ \big(\,(a_1, \dots, a_{p_a})\,,\,(b_1, \dots, b_{v-p_a-1}, b_{v-p_a+1}, \dots, b_{p_b})\,\big) & \text{else} \end{cases}.$$

Last, for all $k \in \mathbb{N}$, $\mathscr{L}_k$ refers to the Lebesgue measure on $\mathbb{R}^k$.

Theorem 2 (Consistency of the MAP estimator) *Assume that there exists an integer $\ell \in [\![1,n]\!]$ such that:*

- (H 1) *The number of observations is bigger than the one of latent variables: $p^\ell < k^\ell$ where $k^\ell = \sum_{i=1}^{\ell} k_i$ and $p^\ell = p_{pop} + \ell\, p_{ind}$;*
- (H 2) *The times of registration $\boldsymbol{t}_i = (t_{i,j})_{j\in[\![1,k_i]\!]}$ are independent and identically distributed;*
- (H 3) *The density $P(\mathrm{d}\boldsymbol{y}^\ell)$ is continuous with polynomial tail decay of degree bigger than the dimension of the truncated space of latent variables, i.e. bigger than $p^\ell + 1$, apart from a subset compact K of $\mathbb{R}^{k^\ell}$;*

(H 4) *The individual trajectories grow super-linearly with respect to the regular variables: for all individuals* $i \in [\![1, n]\!]$ *and for all* $v \in [\![1, p_{pop}^{reg} + p_{ind}^{reg}]\!]$*, there exists two functions* $a_{i,v}, b_{i,v} \colon \mathbb{R}^{p_{pop}^{reg}+p_{ind}^{reg}-1} \to \mathbb{R}$ *which depend only of* $(\boldsymbol{z}_{pop}^{reg}, \boldsymbol{z}_i^{reg})_{-v}$ *and such that for all* $(\boldsymbol{z}_{pop}, \boldsymbol{z}_i) \in \mathcal{Z}_{pop} \times \mathcal{Z}_i$*,*

$$a_{i,v}\left((\boldsymbol{z}_{pop}^{reg}, \boldsymbol{z}_i^{reg})_{-v}\right) \geqslant 0 \quad \textit{where} \quad a_{i,v}\left((\boldsymbol{z}_{pop}^{reg}, \boldsymbol{z}_i^{reg})_{-v}\right) = 0 \quad \textit{iff} \quad (\boldsymbol{z}_{pop}^{reg}, \boldsymbol{z}_i^{reg})_{-v} = 0$$

$$\textit{and} \quad \|\vec{\boldsymbol{\gamma}}_{\boldsymbol{i}}(\boldsymbol{z}_{pop}, \boldsymbol{z}_i)\|_\infty \geqslant a_{i,v}\left((\boldsymbol{z}_{pop}^{reg}, \boldsymbol{z}_i^{reg})_{-v}\right)\left|(\boldsymbol{z}_{pop}^{reg}, \boldsymbol{z}_i^{reg})_{v}\right| + b_{i,v}\left((\boldsymbol{z}_{pop}^{reg}, \boldsymbol{z}_i^{reg})_{-v}\right) ;$$

(H 5) *Critical variables induce critical trajectories: for all individuals* $i \in [\![1, n]\!]$ *and for all* $v \in [\![1, p_{pop}^{crit} + p_{ind}^{crit}]\!]$*, there exists a critical trajectory* $\gamma_{i,v}^{crit}$

$$\lim_{\left|(\boldsymbol{z}_{pop}^{crit}, \boldsymbol{z}_i^{crit})_v\right| \to +\infty} \vec{\boldsymbol{\gamma}}_i(\boldsymbol{z}_{pop}, \boldsymbol{z}_i) = \gamma_{i,v}^{crit} \qquad \textit{and} \qquad \mathscr{L}_{k_i}(\{y_i = \gamma_{i,v}^{crit}\}) = 0\,.$$

Let $(\hat{\theta}_n)_{n\in\mathbb{N}}$ *denote any* MAP *estimator. Then* $\Theta_*^\omega \neq \varnothing$ *and for any* $\varepsilon \in \mathbb{R}_+^*$*,*

$$\lim_{n\to\infty} \mathbb{P}\left[\delta(\hat{\theta}_n, \Theta_*^\omega) \geqslant \varepsilon\right] = 0$$

where δ *in any metric compatible with the topology on* Θ^ω*.*

See Appendix A for the proof.

If the times of observations $\boldsymbol{t}_i$ are identically distributed, the individual numbers of measurements k_i are in particular all equal. Thus, under (H 2), Assumption (H 1) writes in a more concise manner as $p^\ell < \ell\, k_1$. However, as (H 2) is not required for all intermediate results (see the proof, Appendix A), we keep the more general statement for (H 1). This condition is for instance met if we assume that the times $\boldsymbol{t}_i$ are regularly spaced, that is to say that for all individuals $i \in [\![1, n]\!]$ and all measurements $j \in [\![1, k_1]\!]$, $t_{i,j}$ follows the uniform distribution $\mathcal{U}([T_{j-1}, T_j])$, where T is a maximum of the set $\{t_{i,j} | i \in [\![1, n]\!],\ j \in [\![1, k_1]\!]\}$ and $(T_0 = 0 < T_1 < \ldots < T_{k_1} = T)$ is a subdivision of $[0, T]$.

The condition $p^\ell < k^\ell$ means that without enough observations for at least some individuals, we cannot build a consistent model. Such an assumption is quite reasonable as we have no chance to catch the trajectories behavior with certitude with less observations than the constraints over them. The assumption on the distribution $P(\mathrm{d}\boldsymbol{y})$ is really weak and always fulfilled in practice. Moreover, as the theorem holds for all $\omega \in \mathbb{R}^+$, the boundary over the average of the population latent variable $\overline{\boldsymbol{z}_{\mathrm{pop}}}$ is not really restrictive.

For compactness, we have stated the theorem by considering that a latent variable may be of only one kind: regular or critical. Actually, a single latent variable can be of two kinds: critical in the neighbourhood of $+\infty$ and regular around $-\infty$, and *vice-versa* (see the proof for details). This remark is all the more important in view of some applications and Section 4 but can be treated by our proof.

3.3 Estimation with the MCMC-SAEM Algorithm

As explain at the paragraph 2.3.2, a stochastic version of the EM algorithm is adopted, namely the SAEM algorithm. As the conditional distribution $q(\boldsymbol{z}|\boldsymbol{y}, \theta)$ is unknown, the

simulation step is replaced using a sampling algorithm, leading to consider the MCMC-SAEM algorithm. It alternates between simulation, stochastic approximation and maximization steps until convergence. The simulation step is achieved using a symmetric random walk Hasting-Metropolis within Gibbs sampler (Robert and Casella, 1999).

The complete log-likelihood of our model writes

$$\begin{aligned}\log q\big(\boldsymbol{y},\boldsymbol{z},\theta\big) \;=\; & -\frac{1}{2\sigma^2}\sum_{i=1}^{n}\sum_{j=1}^{k_i}\big(\,y_{i,j}-\gamma_i(t_{i,j})\,\big)^2 - k\log(\sigma) - \frac{1}{2}\sum_{i=1}^{n}\big({}^t\boldsymbol{z}_i\,\Sigma^{-1}\,\boldsymbol{z}_i\big) - \frac{n}{2}\log(|\Sigma|)\\ & - \frac{1}{2}\,{}^t\big(\,\boldsymbol{z}_{\rm pop}-\overline{\boldsymbol{z}_{\rm pop}}\,\big)D^{-1}\big(\,\boldsymbol{z}_{\rm pop}-\overline{\boldsymbol{z}_{\rm pop}}\,\big) - \frac{1}{2}\log(|D|) - \frac{1}{2}\,\mathrm{tr}\left(V\Sigma^{-1}\right)\\ & + \frac{m_\Sigma}{2}\big(\,\log(|V|)-\log(|\Sigma|)\,\big) + m_\sigma\log\left(\frac{v}{\sigma}\right) - \frac{m_\sigma}{2}\left(\frac{v}{\sigma}\right)^2 + \,csts\,.\end{aligned}$$

It is clear to see that this model belongs to the curved exponential family: the sufficient statistics may for instance be defined as

$$\boldsymbol{S}_1(\boldsymbol{y},\boldsymbol{z}) = \boldsymbol{z}_{\rm pop} \quad ; \quad S_2(\boldsymbol{y},\boldsymbol{z}) = \frac{1}{n}\sum_{i=1}^{n}{}^t\boldsymbol{z}_i\boldsymbol{z}_i \quad ; \quad S_3(\boldsymbol{y},\boldsymbol{z}) = \frac{1}{k}\sum_{i=1}^{n}\sum_{j=1}^{k_i}\big(\,y_{i,j}-\gamma_i(t_{i,j})\,\big)^2$$

where $\boldsymbol{S}_1(\boldsymbol{y},\boldsymbol{z}) \in \mathbb{R}^{p_{\rm pop}}$, $S_2(\boldsymbol{y},\boldsymbol{z}) \in \mathscr{M}_{p_{\rm ind}}(\mathbb{R})$ and $S_3(\boldsymbol{y},\boldsymbol{z}) \in \mathbb{R}$.

The maximization step is straightforward given the sufficient statistics of our exponential model: we update the parameters by taking a barycentre between the corresponding sufficient statistic and the prior (when there exists). In other words, by denoting $\texttt{iter}$ the increment: $\overline{\boldsymbol{z}_{\rm pop}}^{(\texttt{iter}+1)} = \boldsymbol{S}_1(\boldsymbol{y},\boldsymbol{z}^{(\texttt{iter})})$,

$$\Sigma^{(\texttt{iter}+1)} = \frac{nS_2(\boldsymbol{y},\boldsymbol{z}^{(\texttt{iter})}) + m_\Sigma V}{n+m_\Sigma} \qquad \text{and} \qquad \sigma^{2(\texttt{iter}+1)} = \frac{kS_3(\boldsymbol{y},\boldsymbol{z}^{(\texttt{iter})}) + m_\sigma v^2}{k+m_\sigma}\,.$$

Finally, given an adapted sampler and the sequence $(\varepsilon_{\texttt{iter}})_{\texttt{iter}>0}$ defined by

$$\forall\,\texttt{iter} \geqslant 1, \quad \varepsilon_{\texttt{iter}} \;=\; \mathbb{1}_{\texttt{iter}\leqslant\texttt{Nburnin}} \;+\; (\texttt{iter}-\texttt{Nburnin})^{-0.65}\,\mathbb{1}_{\texttt{iter}>\texttt{Nburnin}}$$

our algorithm writes as Algorithm 1 . Some experimental results are presented in Section 5.

4. Example of the Piecewise-Logistic Curve Model

In this section, we explicit the generic model with logistic geodesics and $M =]0,1[$. This is motivated by the study of the RECIST score monitoring, which leads to consider one-dimension manifold, with one rupture point. As this explicit model is designed in view of our target application, we first give a short description of RECIST score.

4.1 Motivation: Chemotherapy Monitoring through RECIST Score

Patients suffering from the metastatic kidney cancer, take a drug each day and regularly have to check their tumor evolution. Indeed, during the past few years, the way we treat renal metastatic cancer was profoundly changed: a new class of anti-angiogenic therapies

Algorithm 1: Overview of the SAEM for the generic piecewise-geodesic model.

Input: $\theta^* = (\overline{\boldsymbol{z}_{\text{pop}}}^*, \Sigma^*, \sigma^*)$, (V, m_Σ), (v, m_σ), `maxIter`, `Nburnin`.

Output: $\theta = (\overline{\boldsymbol{z}_{\text{pop}}}, \Sigma, \sigma)$.

```
# Initialization: θ ← θ* ;  S ← 0 ;  (ε_iter)_{iter>0} ;  z_pop ← z̄_pop ;  (z_i)_i ← 0 ;
for iter = 1 to maxIter do
    # Simulation: (z_pop, (z_i)_i) ← sampler(z_pop, (z_i)_i) ;
    # Stochastic Approximation: S_1 ← S_1 + ε_iter (z_pop − S_1) ;
        S_2 ← S_2 + ε_iter ( (1/n) Σ_i ᵗz_i z_i − S_2 ) ;
        S_3 ← S_3 + ε_iter ( (1/k) Σ_{i=1}^{n} Σ_{j=1}^{k_i} ( y_{i,j} − γ_i(t_{i,j}) )² − S_3 ) ;
    # Maximization: z̄_pop ← S_1 ;  Σ ← (nS_2 + m_Σ V)/(n + m_Σ) ;  σ ← sqrt( (kS_3 + m_σ v²)/(k + m_σ) ) ;
end
```

targeting the tumor vessels instead of the tumor cells has emerged and drastically improved survival by a factor of three (Escudier et al., 2016). These new drugs, however, do not cure the cancer, and only succeed in delaying the tumor growth, requiring the use of successive therapies which must be continued or interrupted at the appropriate moment according to the patient's response. So, the new medicine process has also created a new scientific challenge: how to choose the most efficient drug therapy.

The RECIST (Response Evaluation Criteria In Solid Tumors) score (Therasse et al., 2000) is a set of published rules that measures the tumoral growth. Physicians select at most five lesions, with a sufficient diameter, and sum the longest diameter for all target lesions. This leads them to determine if the tumors in cancer patients respond (completely or partially), stabilize or progress during treatment.

The response to a given treatment has generally two distinct phases: first, tumor's size reduces; then, the tumor grows again. So, we have to build a model which allow to us to catch this behaviors. Moreover, a practical question is to quantify the correlation between both phases and to determine as accurately as possible the individual rupture times t_R^i which are related to an escape of the patient's response to treatment.

4.2 The Piecewise-Logistic Curve Model

Our observations consist of patient's RECIST score over time, *i.e.* of sequences of bounded one-dimension measures. As explained above, we could make out two phases in the evolution of RECIST scores: a decreasing and a growing one. So, we set $m = 2$ and $d = 1$, which leads us to propose a way to build models for chemotherapy monitoring. This model has been designed after discussions with oncologists of the HEGP.

4.2.1 The Group-Representative Trajectory

Let M_0 be the open interval $]0, 1[$, equipped with the logistic metric

$$\forall x \in M_0, \quad \forall \xi, \zeta \in T_x M_0 \simeq \mathbb{R}, \quad g_x(\xi, \zeta) = \xi \, \mathcal{G}(x) \, \zeta \quad \text{with} \quad \mathcal{G}(x) = \frac{1}{x^2(1-x^2)} \, .$$

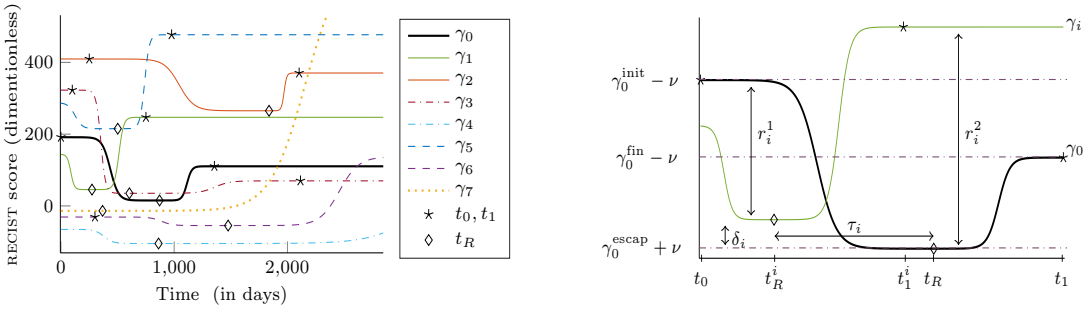

(a) Diversity of individual trajectories.

(b) From representative to individual trajectory.

Figure 1: *Model description.* Figure 1a represents a typical representative trajectory in bold and several individual ones, for different vectors $\boldsymbol{z}_i$. The rupture times are represented by diamonds and the initial/final times by stars. Figure 1b illustrates the non-standard constraints for γ_0 and the transition from the representative trajectory to an individual one: the trajectory γ_i is subject to a temporal and a spacial warp. In other "words", $\gamma_i = \phi_i^1 \circ \gamma_0^1 \circ \psi_i^1 \, \mathbb{1}_{]-\infty, t_R^i]} + \phi_i^2 \circ \gamma_0^2 \circ \psi_i^2 \, \mathbb{1}_{]t_R^i, +\infty[}$.

Given three real numbers γ_0^{init}, γ_0^{escap} and γ_0^{fin} we define two affine functions by setting down $\phi_0^1 \colon x \mapsto \left(\gamma_0^{\text{init}} - \gamma_0^{\text{escap}}\right) x + \gamma_0^{\text{escap}}$ and $\phi_0^2 \colon x \mapsto \left(\gamma_0^{\text{fin}} - \gamma_0^{\text{escap}}\right) x + \gamma_0^{\text{escap}}$. This allows us to map M_0 onto the intervals $]\gamma_0^{\text{escap}}, \gamma_0^{\text{init}}[$ and $]\gamma_0^{\text{escap}}, \gamma_0^{\text{fin}}[$ respectively: if $\bar{\gamma}_0$ refers to the sigmoid function, $\phi_0^1 \circ \bar{\gamma}_0$ will be a logistic curve, growing from γ_0^{escap} to γ_0^{init}. For compactness, we note t_R the single breaking-up time at the population level and t_R^i at the individual one. Moreover, due to our target application, we force the first logistic to be decreasing and the second one increasing (this condition may be easily relaxed for other framework).

Logistics are defined on open intervals, with asymptotic constraints. We want to formulate our constraints on some non-infinite time-points, as explained in paragraph 2.1.2. So, we set a positive threshold ν, close to zero, and demand the logistics γ_0^1 and γ_0^2 to be ν-near from their corresponding asymptotes. More precisely, we impose the trajectory γ_0 to be of the form $\gamma_0 = \gamma_0^1 \, \mathbb{1}_{]-\infty, t_R]} + \gamma_0^2 \, \mathbb{1}_{]t_R, +\infty[}$ where, for all time $t \in \mathbb{R}$,

$$\gamma_0^1(t) = \frac{\gamma_0^{\text{init}} + \gamma_0^{\text{escap}} \mathrm{e}^{(at+b)}}{1 + \mathrm{e}^{(at+b)}} \in]\gamma_0^{\text{escap}}, \gamma_0^{\text{init}}[\quad , \quad \gamma_0^2(t) = \frac{\gamma_0^{\text{fin}} + \gamma_0^{\text{escap}} \mathrm{e}^{-(ct+d)}}{1 + \mathrm{e}^{-(ct+d)}} \in]\gamma_0^{\text{escap}}, \gamma_0^{\text{fin}}[$$

and a, b, c and d are some positive numbers given by the following constraints

$$\gamma_0^1(t_0) = \gamma_0^{\text{init}} - \nu \, , \quad \gamma_0^1(t_R) = \gamma_0^2(t_R) = \gamma_0^{\text{escap}} + \nu \quad \text{and} \quad \gamma_0^2(t_1) = \gamma_0^{\text{fin}} - \nu \, .$$

In order the previous logistics to be well-defined, we also have to enforce $\gamma_0^{\text{escap}} + 2\nu \leqslant \gamma_0^{\text{init}}$ and $\gamma_0^{\text{escap}} + 2\nu \leqslant \gamma_0^{\text{fin}}$. Thus, $p_{\text{pop}} = 5$ and

$$\mathcal{Z}_{\text{pop}} = \left\{ \left(\gamma_0^{\text{init}}, \gamma_0^{\text{escap}}, \gamma_0^{\text{fin}}, t_R, t_1 \right) \in \mathbb{R}^5 \;\middle|\; \gamma_0^{\text{escap}} + 2\nu \leqslant \gamma_0^{\text{init}} \;\wedge\; \gamma_0^{\text{escap}} + 2\nu \leqslant \gamma_0^{\text{fin}} \right\} .$$

In our context, the initial time of the process is known: it is the beginning of the treatment. So, we assume that the representative initial time t_0 is equal to zero.

4.2.2 Individual Trajectories

For each subject $i \in [\![1,n]\!]$, given $(\alpha_i^1, \alpha_i^2, \tau_i) \in \mathbb{R}_+^2 \times \mathbb{R}$, the time-warps (*cf.* 2.2.1) write $\psi_i^1(t) = \alpha_i^1(t - t_0 - \tau_i) + t_0$ and $\psi_i^2(t) = \alpha_i^2(t - t_R - \tau_i^2) + t_R$ where $\tau_i^2 = \tau_i^1 + \left(\frac{1-\alpha_i^1}{\alpha_i^1}\right)(t_R - t_0)$.

In the same way as the time-warp, the diffeomorphisms ϕ_i^1 and ϕ_i^2 (*cf.* 2.2.2) are chosen to allow different amplitudes and rupture values: for each $i \in [\![1,n]\!]$, given the two scaling factors r_i^1 and r_i^2 and the space-shift δ_i, we define $\phi_i^\ell(x) = r_i^\ell\,(x - \gamma_0(t_R)) + \gamma_0(t_R) + \delta_i$, $\ell \in \{1,2\}$. Other choices are conceivable but in the context of our target applications, this one is the most appropriate: as we want to study the correlation between growth and decrease phase, none of the portions of the curves have to be favoured and affine functions allow us to put the same weight on the whole curves. Mathematically, any regular and injective function defined on $]\gamma_0^{\text{escap}}, \gamma_0^{\text{init}}[$ (respectively $]\gamma_0^{\text{escap}}, \gamma_0^{\text{fin}}[$) is suited.

To sum up, each individual trajectory γ_i depends on the representative curve γ_0 through fixed $\boldsymbol{z}_{\text{pop}} = \left(\gamma_0^{\text{init}}, \gamma_0^{\text{escap}}, \gamma_0^{\text{fin}}, t_R, t_1\right)$ and random $\boldsymbol{z}_i = \left(\alpha_i^1, \alpha_i^2, \tau_i, r_i^1, r_i^2, \delta_i\right)$ effects. This leads to a non-linear mixed-effects model. More precisely, we set for all individual $i \in [\![1,n]\!]$ $\gamma_i^1 = \phi_i^1 \circ \gamma_0^1 \circ \psi_i^1$, $\gamma_i^2 = \phi_i^2 \circ \gamma_0^2 \circ \psi_i^2$ and $t_R^i = t_0 + \tau_i^1 + \frac{t_R - t_0}{\alpha_i^1}$, which leads us to write for all "time" of measurement $j \in [\![1,k_i]\!]$,

$$
\begin{aligned}
y_{i,j} \;=\; & \left[\, r_i^1 \left(\gamma_i^1(t_{i,j}) - \gamma_0(t_R)\right) + \gamma_0(t_R) + \delta_i \,\right] \mathbb{1}_{]-\infty, t_R^i]}(t_{i,j}) \\
& + \left[\, r_i^2 \left(\gamma_i^2(t_{i,j}) - \gamma_0(t_R)\right) + \gamma_0(t_R) + \delta_i \,\right] \mathbb{1}_{]t_R^i, +\infty[}(t_{i,j}) \;+\; \varepsilon_{i,j}\,.
\end{aligned}
$$

Figure 1 provides an illustration of the model. On each subfigure, the bold black curve represents the characteristic trajectory γ_0 and the colour curves several individual trajectories.

We proceed as in the paragraph 2.3.1 and set $\alpha_i^\ell = \mathrm{e}^{\xi_i^\ell}$ for $\ell \in \{1,2\}$. Likewise, the scaling parameters r_i^ℓ have to be positive and equal to one on average while the space shifts δ_i can be of any signs and must be zero on average. So, we set $r_i^\ell = \mathrm{e}^{\rho_i^\ell}$ for $\ell \in \{1,2\}$ leading to $\boldsymbol{z}_i = \left(\xi_i^1, \xi_i^2, \tau_i, \rho_i^1, \rho_i^2, \delta_i\right)$. In particular, $p_{\text{ind}} = 6$ and we assume that there exists $\Sigma \in \mathscr{S}_{p_{\text{ind}}}^+(\mathbb{R})$ such that $\boldsymbol{z}_i \sim \mathcal{N}(0, \Sigma)$ for all $i \in [\![1,n]\!]$. This assumption is really important: usually, the random effects are studied independently. Here, we are interested in correlations between the two phases of patient's response to treatment.

4.3 Theoretical Analysis of the Piecewise-Logistic Curve Model

Theorem 1 applies as is and the MAP estimator for the piecewise-logistic model is well-defined. Moreover, at the risk of assuming some restriction concerning the distribution of our observations, the piecewise-logistic model is consistent.

More precisely, let Θ^{PL} be the space of the admissible parameters for the piecewise-logistic model, *i.e.* $\Theta^{\text{PL}} = \{\, (\overline{\gamma_0^{\text{init}}}, \overline{\gamma_0^{\text{escap}}}, \overline{\gamma_0^{\text{fin}}}, \overline{t_R}, \overline{t_1}, \Sigma, \sigma) \in \mathbb{R}^{p_{\text{pop}}} \times \mathscr{S}_{p_{\text{ind}}}^+(\mathbb{R}) \times \mathbb{R}^+ \,\}$. We define $\Theta^{\omega,\text{PL}} = \{\, \theta \in \Theta^{\text{PL}} \mid \|(\overline{\gamma_0^{\text{init}}}, \overline{\gamma_0^{\text{escap}}}, \overline{\gamma_0^{\text{fin}}}, \overline{t_R}, \overline{t_1})\| \leqslant \omega \,\}$ the space of the parameters associated to bounded on average fixed effects, for the piecewise-logistic model and, as in the generic framework, the space $\Theta_*^{\omega,\text{PL}} = \{\theta \in \Theta^{\omega,\text{PL}} \mid \mathbb{E}_{P(\mathrm{d}\boldsymbol{y}^\ell)}\left[\log q(\boldsymbol{y}^\ell|\theta)\right] = \mathbb{E}^*(\omega)\}$ where $\mathbb{E}^*(\omega) = \sup_{\theta \in \Theta^{\omega,\text{PL}}} \mathbb{E}_{P(\mathrm{d}\boldsymbol{y}^\ell)}\left[\log q(\boldsymbol{y}^\ell|\theta)\right]$.

Theorem 3 (Consistency of the MAP, piecewise-logistic model) *Assume that*

(H 1) *The number of observations is bigger than the one of latent variables: There exists* $\ell \in [\![1, n]\!]$ *such that* $p^\ell < k^\ell$ *where* $k^\ell = \sum_{i=1}^{\ell} k_i$ *and* $p^\ell = p_{pop} + \ell\, p_{ind}$ *;*

(H 2) *The times of registration* $t_i = (t_{i,j})_{j \in [\![1,k_i]\!]}$ *are independent and identically distributed;*

(H 3) *The density* $P(\mathrm{d}\boldsymbol{y}^\ell)$ *is continuous with polynomial tail decay of degree bigger* $p^\ell + 1$ *apart from a subset compact* K *of* $\mathbb{R}^{k^\ell}$*;*

Then, the piecewise-logistic model satisfies the hypothesis of Theorem 2. In particular, if $(\hat{\theta}_n)_{n\in\mathbb{N}}$ *denote any* MAP *estimator,* $\Theta_*^{\omega,\mathrm{PL}} \neq \varnothing$ *and for any* $\varepsilon \in \mathbb{R}_+^*$*,*

$$\lim_{n\to\infty} \mathbb{P}\left[\delta(\hat{\theta}_n, \Theta_*^{\omega,\mathrm{PL}}) \geqslant \varepsilon\right] = 0$$

where δ *in any metric compatible with the topology on* $\Theta^{\omega,\mathrm{PL}}$*.*

Proof We demonstrate that, for all $i \in [\![1, n]\!]$, the variables $\left(t_R,\, t_1,\, \xi_i^1,\, \xi_i^2,\, \tau_i\right)$ are critical, that $\left(\gamma_0^{\mathrm{init}},\, \gamma_0^{\mathrm{escap}},\, \gamma_0^{\mathrm{fin}},\, \rho_i^1,\, \rho_i^2,\, \delta_i\right)$ are regular and that $\left(\rho_i^1,\, \rho_i^2\right)$ are regular in the neighbourhood of $+\infty$ and critical near $-\infty$. See the remark after Theorem 2.

(H 4) Let $i \in [\![1, n]\!]$. By definition of $\vec{\boldsymbol{\gamma}}_i$,

$$\|\vec{\boldsymbol{\gamma}}_i(\boldsymbol{z}_{\mathrm{pop}}, \boldsymbol{z}_i)\|_\infty = \max\left\{ \begin{array}{l} |\, \gamma_0^{\mathrm{escap}} + \nu + \delta_i\,| \\ |\, \gamma_0^{\mathrm{escap}} + \nu + \delta_i + \mathrm{e}^{\rho_i^1}(\gamma_0^{\mathrm{init}} - \gamma_0^{\mathrm{escap}} - 2\nu)\,| \\ |\, \gamma_0^{\mathrm{escap}} + \nu + \delta_i + \mathrm{e}^{\rho_i^2}(\gamma_0^{\mathrm{fin}} - \gamma_0^{\mathrm{escap}} - 2\nu)\,| \end{array} \right\}.$$

And we can check that for γ_0^{init}, $\gamma_0^{\mathrm{escap}}$, γ_0^{fin}, ρ_i^1, ρ_i^2 and δ_i and that for ρ_i^1 and ρ_i^2 as soon as $|\rho_i^1|, |\rho_i^2| \geqslant 1$ there exists two functions a_i and b_i as in [Theorem 2(H 4)].

(H 5) Let $i \in [\![1, n]\!]$ and $j \in [\![1, k_i]\!]$. By definition of $\vec{\boldsymbol{\gamma}}_i$,

$$\lim_{t_R\to+\infty} \vec{\boldsymbol{\gamma}}_i(\boldsymbol{z}_{\mathrm{pop}}, \boldsymbol{z}_i)_j = \left[\, \mathrm{e}^{\rho_i^1}\left(\gamma_0^{\mathrm{init}} - \gamma_0^{\mathrm{escap}} - 2\nu\right) + \gamma_0^{\mathrm{escap}} + \nu + \delta_i \,\right] \mathbb{1}_{[t_0,+\infty[}(t_{i,j})$$

where $\vec{\boldsymbol{\gamma}}_i(\boldsymbol{z}_{\mathrm{pop}}, \boldsymbol{z}_i)_j$ denotes the j^{th} coordinate of the vector $\vec{\boldsymbol{\gamma}}_i(\boldsymbol{z}_{\mathrm{pop}}, \boldsymbol{z}_i) \in \mathbb{R}^{k_i}$. However, by construction, $\gamma_0^{\mathrm{init}} - \gamma_0^{\mathrm{escap}}$ and $\gamma_0^{\mathrm{escap}}$ follow a normal distribution so

$$\mathscr{L}_{k_i}\left(\left\{\, y_{i,j} = \mathrm{e}^{\rho_i^1}\left(\gamma_0^{\mathrm{init}} - \gamma_0^{\mathrm{escap}} - 2\nu\right) + \gamma_0^{\mathrm{escap}} + \nu + \delta_i \,\right\}\right) = 0\,.$$

Likewise for $t_R \to -\infty$. The same argument holds when t_1, ξ_i^1, ξ_i^2 or τ_i become infinite and when ρ_i^1 or ρ_i^2 go to $-\infty$.

■

5. Experimental Results

Experimentations are performed for the piecewise-logistic curve model introduced above. In order to validate our model and numerical scheme, we first run experiments on synthetic data. We then test our estimation algorithm on real data from the HEGP. A medical paper is under progress to provide a more accurate interpretation of this results.

5.1 Synthetic Data

We generate four types of data set, to put our algorithm in different situations. More precisely, we want to quantify its sensitivity to initialisation, sample size and noise.

5.1.1 Influence of the Initialization

The estimation is performed through the SAEM algorithm (Algorithm 1). This iterative algorithm is proven to converge toward a critical point of the observed likelihood. Therefore, as our model does no imply a convex likelihood, one may end up with a local *maximum* depending on the initialization point and the dynamic of our iterations. This choice of initialization appears crucial. In particular the choice of the initial mean population parameters $\overline{\boldsymbol{z}_{\text{pop}}}^{\text{init}}$ as illustrated bellow.

If our model were linear, the representative curve γ_0 would exactly be the one induced by the mean of the individual trajectories γ_i, *i.e.* the one where $\boldsymbol{z}_{\text{pop}} = \text{mean}_{i\in[\![1,n]\!]}\ \boldsymbol{z}_i$. Following this idea, we set in our experiments

$$\overline{\gamma_0^{\text{init}}}^{\text{init}} = \underset{i\in[\![1,n]\!]}{\text{mean}}\ y_{i,1} \quad ; \quad \overline{\gamma_0^{\text{escap}}}^{\text{init}} = \underset{i\in[\![1,n]\!]}{\text{mean}}\ \underset{j\in[\![1,k_i]\!]}{\min}\ y_{i,j} \quad ; \quad \overline{\gamma_0^{\text{fin}}}^{\text{init}} = \underset{i\in[\![1,n]\!]}{\text{mean}}\ y_{i,k_i} \quad ;$$

$$\overline{t_R}^{\text{init}} = \frac{1}{2}\ \underset{i\in[\![1,n]\!]}{\text{mean}}\ t_{k_i} \qquad \text{and} \qquad \overline{t_1}^{\text{init}} = \underset{i\in[\![1,n]\!]}{\text{mean}}\ t_{k_i}\ .$$

Note that the choice of the initial covariance matrix Σ^{init} and the residual noise σ^{init} does not seem to be very influential. We just demand Σ^{init} to be definite positive.

5.1.2 Influence of the Proposal Variances

The SAEM algorithm is very sensitive to the choice of the proposal variances in the sampling step. Thus, we have to carefully tune these variances in order the mean acceptance ratio to stay around the optimal rate – 24% as we are using a symmetric random walk sampler. To decrease the influence of a bad calibration, we adapt the proposal variances over the iterations in the way of Roberts and Rosenthal (2007, 2009): every s^{th} batch of 50 iterations, we increase or decrease the logarithm of the proposal proposal variances by $\delta(s) = \min\left(0.001, \frac{1}{\sqrt{s}}\right)$ depending on whether the mean associated variable acceptance rate is bigger or smaller than the optimal one. Note that we have also tried to adapt the proposal variances as in Atchadé (2006) but the results we obtained were not satisfactory. Actually, it appears numerically that if we want the adaptive procedure to increase the efficiency of our algorithm, we must modify the proposal variance neither too often nor with a too big amplitude of change.

Table 1: *Degree of non-linearity*: Relative errors (expressed as a percentage) for the initial population parameters $\overline{\boldsymbol{z}_{\text{pop}}}^{\text{init}}$ and residual noise σ^{true} used to generate the data set, according to the type of data set and the sample size n.

	n	$\Delta_{\mathscr{L}}(\overline{\gamma_0^{\text{init}}})$	$\Delta_{\mathscr{L}}(\overline{\gamma_0^{\text{escap}}})$	$\Delta_{\mathscr{L}}(\overline{\gamma_0^{\text{fin}}})$	$\Delta_{\mathscr{L}}(\overline{t_R})$	$\Delta_{\mathscr{L}}(\overline{t_1})$	σ
A	50	7.08	17.01	5.94	1.97	1.98	1.99
	100	2.93	22.33	3.66	2.40	2.42	1.99
	250	2.16	24.06	2.12	3.52	3.54	1.99
A*	50	5.63	283.14	1.51	1.03	1.01	20.09
	100	3.38	259.25	0.07	4.75	4.76	20.09
	250	3.67	269.42	0.41	3.94	3.95	20.09
B	50	80.47	2.77	39.78	35.04	35.09	0.29
	100	88.17	4.39	51.83	36.14	36.19	0.29
	250	83.52	12.91	47.90	33.23	33.27	0.29
B*	50	59.25	201.98	33.46	28.85	28.89	20.86
	100	74.94	213.96	43.50	30.74	30.78	20.86
	250	79.14	229.40	47.30	34.39	34.44	20.86

5.1.3 Construction of the Data Sets

For each type of data set, given the corresponding ground truth parameters θ^{true}, we generate three data sets of respective size 50, 100 and 250. Last, to put our algorithm on a more realistic situation, the synthetic individual times are non-periodically spaced and individual sizes vary between 12 and 18.

The first type – A – is said quasilinear in the sense that, for these data sets, the representative trajectory γ_0 is "close" to the mean trajectory described above. Hence, we put our algorithm in a favourable situation where the optimal representative trajectory is close to the initial one. The second type –A* – is a noisy version of A.

On the contrary, the thirds type – B – is built in order to be "truly non-linear": the representative trajectory γ_0 is "far" from the curve built by $\overline{\boldsymbol{z}_{\text{pop}}}^{\text{init}}$. Likewise, the fourth type – B* – is a noisy version of B. To measure this degree of non-linearity, we introduce the ratio $\Delta_{\mathscr{L}}(\overline{\boldsymbol{z}_{\text{pop}}})$ which is the relative error of $\overline{\boldsymbol{z}_{\text{pop}}}^{\text{init}}$: $\Delta_{\mathscr{L}}(\overline{\boldsymbol{z}_{\text{pop}}}) = \frac{\|\overline{\boldsymbol{z}_{\text{pop}}}^{\text{init}} - \overline{\boldsymbol{z}_{\text{pop}}}^{\text{true}}\|}{\|\overline{\boldsymbol{z}_{\text{pop}}}^{\text{init}}\|}$. Table 1 compiles this ratio for every data set, and for every parameter in $\overline{\boldsymbol{z}_{\text{pop}}}$.

5.1.4 Estimation of the Fixed Effects

Table 2 displays the relative errors for the estimated population parameters. In most case, these errors decrease with the size of the data set. More specific to our model, we observe that these errors are correlated to the subjective linearity of the model. With the exception of $\overline{\gamma_0^{\text{escap}}}$, the errors for estimating population parameters grow linearly with the non-linearity of the model. We suppose that the difference of scale between $\overline{\gamma_0^{\text{escap}}}$ and the others can, at least partly, explain this phenomena: $\overline{\gamma_0^{\text{escap}}}$ is about a few tens of units ; $\overline{\gamma_0^{\text{init}}}$, $\overline{\gamma_0^{\text{fin}}}$ and $\overline{t_R}$ about a few hundreds and $\overline{t_1}$ about one thousand. Thus, a same absolute error will lead to markedly different relative error.

Table 2: *Fixed effects*: Mean (standard deviation) relative errors (expressed as a percentage) over 50 runs, for the estimated parameters $\overline{\boldsymbol{z}_{\text{pop}}}^{\text{estim}}$, according to the data set and the sample size n.

	n	$\overline{\gamma_0^{\text{init}}}$	$\overline{\gamma_0^{\text{escap}}}$	$\overline{\gamma_0^{\text{fin}}}$	$\overline{t_R}$	$\overline{t_1}$
A	50	6.03 (0.32)	10.25 (0.50)	3.69 (0.25)	1.95 (0.13)	2.43 (0.18)
	100	2.19 (0.17)	3.28 (0.22)	2.07 (0.18)	1.69 (0.11)	1.86 (0.17)
	250	1.30 (0.10)	1.96 (0.13)	1.53 (0.08)	0.78 (0.06)	1.67 (0.09)
A*	50	3.74 (0.26)	25.73 (1.64)	6.84 (0.40)	3.32 (0.26)	3.73 (0.26)
	100	2.35 (0.15)	12.20 (0.64)	1.35 (0.09)	2.98 (0.22)	2.29 (0.18)
	250	1.70 (0.12)	3.94 (0.29)	1.33 (0.09)	1.36 (0.10)	1.51 (0.10)
B	50	71.13 (1.33)	100.24 (8.09)	90.73 (2.54)	7.78 (0.56)	46.39 (1.32)
	100	58.73 (0.98)	58.88 (3.00)	84.99 (1.42)	8.13 (0.57)	42.06 (1.04)
	250	67.49 (0.47)	23.12 (1.54)	57.82 (0.74)	6.01 (0.33)	38.09 (0.36)
B*	50	41.61 (1.26)	29.86 (2.53)	46.38 (1.60)	9.04 (0.58)	29.90 (0.58)
	100	60.39 (0.81)	28.43 (2.06)	58.35 (1.07)	8.11 (0.54)	29.75 (0.50)
	250	55.89 (0.74)	15.56 (0.98)	59.90 (0.58)	3.26 (0.25)	39.28 (0.43)

The degree of non-linearity in the data set seems to play a significant role in the estimation of the population parameters. To be certain that the poor estimation of $\overline{\boldsymbol{z}_{\text{pop}}}$ when the ratio $\Delta_{\mathscr{L}}(\overline{\boldsymbol{z}_{\text{pop}}})$ is too big is due to the non-linearity of the data set and not to a bad initialization, we have also performed estimations by assigning $\theta^{\text{init}} = \theta^{\text{true}}$. The results were better but not so significantly. Despite this limitation, the algorithm we propose is not noise-sensitive: errors for non-noisy and noisy version of a same type of data set are notably the same. Moreover, the population parameters are well-learned in quasilinear cases and in particular in large data set ($n = 250$) and the mean rupture time $\overline{t_R}$ seems to be well-estimated, no matter the subjective linearity of the data set.

5.1.5 Estimation of the Inter-Individual Variability

In the target of our application, the covariance matrix Σ gives a lot of information on the health status of a patient: pace and amplitude of tumor progression, individual rupture times, *etc.* Therefore, we have to pay special attention to the estimation of Σ.

Much as the representative trajectory is not always good-estimated, our algorithm always allows a well-understanding of the inter-individual variability. We present at Table 3 the Kullback-Leibler divergence from Σ^{estim} to Σ^{true}, the relative error of the individual rupture times and the estimated residual noise. As for the estimation of the population parameters, errors decrease with the sample size n and are not significantly different between noisy and non-noisy versions of a same type of data set. Moreover, in that case, the errors seem to not rely on the subjective linearity of the data set.

5.1.6 Reconstruction of the Individual Trajectories

Figure 2 illustrates the well-understanding of the variance within the population, including for the non-linear data set. Determining accurate individual rupture time t_R^i is all the most important as, in the aim of chemotherapy monitoring, these times are related to an escape of the patient's response to treatment.

Table 3: *Variability and residual noise*: Mean (standard deviation) of KullbackLeibler divergences from Σ^{estim} to Σ^{true}, mean (standard deviation) relative errors (expressed as a percentage) for the individual rupture times $t_R^{i\,\text{estim}}$ and mean estimated residual noise σ^{estim} according to the data set and the sample size n. All over 50 runs.

		Type **A**			Type **B**		
	n	Σ	t_R^i	σ	Σ	t_R^i	σ
X	50	15.54 (5.17)	0.49 (0.04)	2.03	16.53 (7.72)	5.89 (3.45)	3.07
	100	8.45 (2.26)	0.63 (0.06)	1.97	13.59 (5.42)	4.44 (1.93)	2.14
	250	9.29 (3.13)	0.57 (0.60)	2.06	22.24 (9.77)	4.96 (1.93)	2.49
$\mathbf{X}^*$	50	16.52 (19.45)	4.66 (0.45)	19.81	27.62 (17.71)	14.32 (4.06)	19.93
	100	12.86 (4.26)	3.85 (0.32)	19.03	23.98 (18.07)	13.97 (3.71)	20.56
	250	6.72 (2.44)	3.98 (0.32)	20.07	17.70 (5.35)	11.57 (2.42)	21.38

An important point was to allow a lot of different individual behaviors. In our synthetic example, Figure 1a illustrates this variability. From a single representative trajectory (γ_0 in bold plain line), we can generate individuals who are cured at the end (dot-dashed lines: γ_3 and γ_4), some whose response to the treatment is bad (dashed lines: γ_5 and γ_6), some who only escape (no positive response to the treatments – dotted lines: γ_7). Likewise, we can generate "patients" with only positive responses or no response at all. The case of individual 4 is interesting in practice: the tumor still grows but so slowly that the growth is negligible, at least in the short-run.

Figure 3 illustrates the qualitative performance of the estimation. We are notably able to understand various behaviors and fit subjects which are far from the characteristic path. Moreover, the noise seems to not reduce the quality of the estimation. We represent only five individuals but 250 subjects have been used to perform the estimation.

5.2 Metastatic Kidney Cancer Monitoring

The algorithm is now run on RECIST score of real patients suffering from kidney cancer. The estimation is performed over a cohort of 176 patients of the HEGP. There is an average of 7 visits per subjects (min: 3, max: 22), with an average duration of 90 days between consecutive visits. We present here a run with a low residual standard variation with respect to the amplitude of the trajectories and complexity of the data set: $\sigma = 9.10$.

Figure 4a illustrates the qualitative performance of the model on ten patients. Although we cannot explain all the paths of progression, the algorithm succeeds in fitting various types of curves: from the curve γ_6 which is flat to the curve γ_3 which is spiky. From Figure 4b, it seems that the rupture times occur early in the progression in average.

In Figure 5, we plot the individual estimates of the random effects (obtained from the last iteration) in comparison to the individual rupture times. Even though the parameters which lead the space warp, *i.e.* ρ_i^1, ρ_i^2 and δ_i are correlated, the correlation with the rupture time is not clear. In other words, the volume of the tumors seems to not be relevant to evaluate the escapement of a patient. On the contrary, which is logical, the time warp strongly impacts the rupture time.

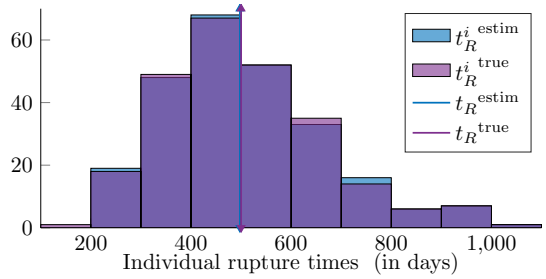

(a) A – *Quasi-linear*

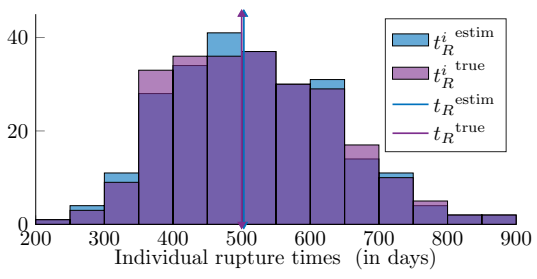

(b) A* – *Noisy and quasi-linear*

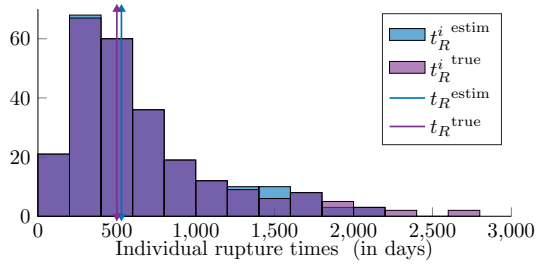

(c) B – *Strongly non-linear*

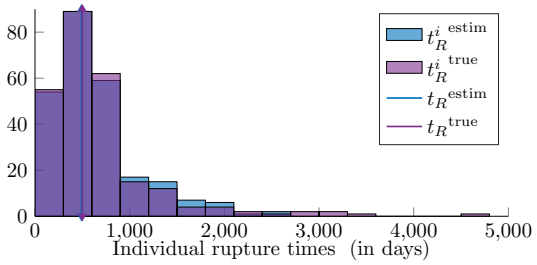

(d) B* – *Noisy and non-linear*

Figure 2: *Distribution of the individual rupture times.* Each subfigure compares the distribution of the (mean of the) estimated individual rupture times $t_R^{i\ \text{estim}}$ and the distribution of the true individual rupture times $t_R^{i\ \text{true}}$. In bold line, the estimated average rupture time t_R^{estim} and the true average rupture time t_R^{true} are relatively close to each other. $n = 250$.

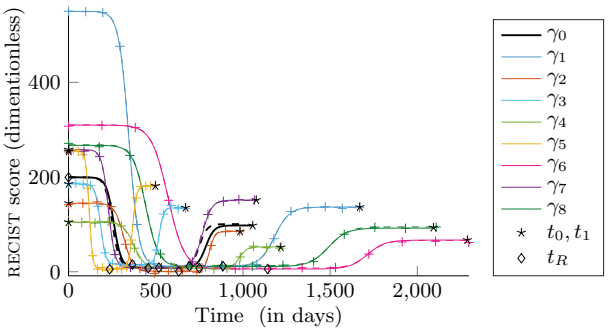

(a) A – *Quasi-linear*

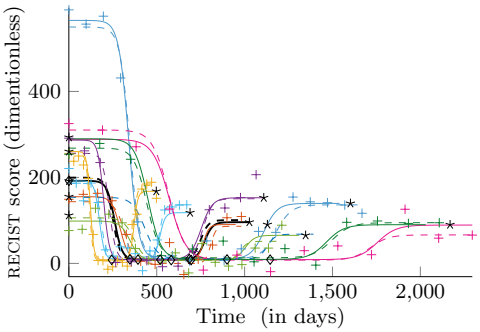

(b) A* – *Noisy and quasi-linear*

Figure 3: *Qualitative performance of the estimation and robustness to noise of the* MAP *estimator.* On both figures, the estimated trajectories are in plain lines and the target curves in dashed lines. The (noisy) observations are represented by crosses. The representative path is in bold black line, the individuals in colour. $n = 250$.

6. Discussion and Perspective

We have proposed a coherent statistical framework for the spatio-temporal analysis of piecewise-geodesic manifold-valued measurements. This model allows each individual to

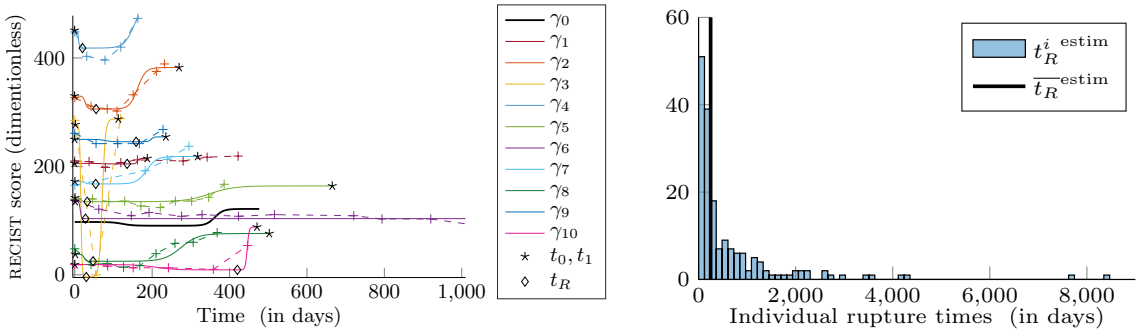

(a) RECIST score of patients from the HEGP. (b) Individual rupture times t_R^i (in days).

Figure 4: RECIST *score*. We keep conventions of the previous figures. We represent at Fig. 4a only 10 patients among the 176. Fig. 4b is the histogram of the rupture times t_R^i for this run. In black bold line, the estimated average rupture time $\overline{t_R}$ is a good estimate of the average of the individual rupture times although there exists a large range of escape.

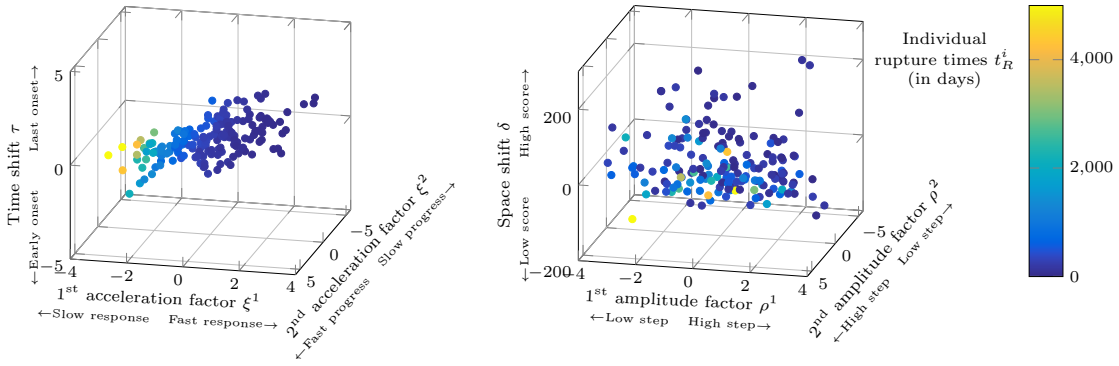

(a) The time warp. (b) The space warp.

Figure 5: *Individual random effects*. Fig. 5a: log-acceleration factors ξ_i^1 and ξ_i^2 against times shifts τ_i. Fig. 5b: log-amplitude factors ρ_i^1 and ρ_i^2 against space shifts δ_i. In both figures, the colour corresponds to the individual rupture time t_R^i. These estimates hold for the same run as Fig. 4.

have his own intrinsic geometry and his own time-parametrization. The model is built in a hierarchical way as a non-linear mixed-effects model whose fixed effects define a representative trajectory of the global evolution in the space of measurements and random effects account for the spatio-temporal variability of the trajectories at the individual level.

Estimation was formulated as a well-defined MAP problem and numerically performed through the MCMC-SAEM algorithm. Experimentations have highlighted the robustness of our model to noise and its performance in catching individual behaviors. We believe that the complexity of our model ensures its practical identifiability, even if it is not structurally identifiable (Lavielle and Aarons, 2016). Besides, as the posterior-likelihood is not convex, the MAP could be difficult to determine numerically. Future work focuses on exploring some possible improvement of the numerical scheme.

Our model can be applied to a wide variety of situations and data sets. In particular, we can address medical follow-up such as neurodegenerative diseases or chemotherapy monitoring. The example of chemotherapy monitoring is especially interesting in a modeling perspective as the patients are treated and tumors may respond, stabilize or progress during the treatment, with different conducts for each phase. At the age of personalized medicine, to give physicians decision support systems is really important. Therefore learning correlations between phases is crucial. This has been taken into account in our experimentations. More generally, the inter-individual variability allows us to personalize the model to new patient and thus perform predictive medicine.

Acknowledgments

Ce travail bénéficie d'un financement public Investissement d'avenir, réference ANR-11 LABX-0056-LMH. This work was supported by a public grant as part of the Investissement d'avenir, project reference ANR-11 LABX-0056-LMH.

Travail réalisé dans le cadre d'un projet financé par la Fondation de la Recherche Médicale DBI20131228564. Work performed as a part of a project funded by the Fondation of Medical Research, grant number DBI20131228564.

Appendix A. Proof of the consistency theorem for bounded population variable

The proof of the theorem relies on several lemmas. Lemma 4 is the heart of the proof: we control here the behavior of the log-likelihood at the boundary points of the parameters space Θ_*^ω and prove that this set is non-empty. It is based on Lemma 3 which states the integrability of the supremum over the parameter space of the positive part of the log-likelihood. Lemma 2 is derived from Allassonnière et al. (2007). We transpose the proof of the cited article here (with few more details) as this lemma is critical in the proof of Lemma 3 and not such classical.

In the following, we freely (and without reminder) use the notations introduced in Section 3.2. Moreover, (H 1), (H 2), (H 3), (H 4) and (H 5) refer to the hypothesis of the consistency theorem (Theorem 2, page 10).

A.1 Lemmas

We first recall that the minimal number of balls of radius $r \in \mathbb{R}_+^*$ required to cover a compact set $K \in \mathbb{R}^p$ is bounded from above by $\left(\frac{\mathcal{D}\text{iam}(K)}{r}\right)^p$.

Lemma 2 (Preliminary of measure theory) *Let $p < q$ be two integers. Then, for any differentiable map $f\colon \mathbb{R}^p \to \mathbb{R}^q$ and any compact subset K of $\mathbb{R}^p$, there exists a constant λ which depends only on p and q such that*

$$\int_{\mathbb{R}^q \setminus f(K)} \log^+ \frac{1}{d\big(\boldsymbol{y}, f(K)\big)} \, \mathrm{d}\boldsymbol{y} \;<\; \lambda \left(\sup_K \|\mathcal{D}f\| + 2\right)^q \mathcal{D}iam(K)^p$$

where d is the euclidean distance on $\mathbb{R}^q$, $\mathcal{D}f$ the differential of f and $\mathcal{D}iam(K)$ the diameter of the compact K. Especially, $\int_{\mathbb{R}^q\setminus f(K)} \log^+ \frac{1}{d(\boldsymbol{y},f(K))}\,\mathrm{d}\boldsymbol{y} < +\infty$.

Proof For all $\rho,\rho_1,\rho_2 \in \mathbb{R}_+^*$, $\rho_1<\rho_2$, let $M_{\rho_1,\rho_2} = \left\{\boldsymbol{y}\in\mathbb{R}^q \mid \rho_1 \leqslant d\big(\boldsymbol{y},f(K)\big) \leqslant \rho_2\right\}$ and $M_\rho = M_{0,\rho}$. For all $\rho\in\mathbb{R}_+^*$, due to the compactness of K, there exists a finite set $\Lambda_\rho\subset K$ such that $K\subset\bigcup_{\boldsymbol{x}\in\Lambda_\rho}\mathcal{B}(\boldsymbol{x},\rho)$ and $|\Lambda_\rho| \leqslant \left(\frac{\mathcal{D}\mathrm{iam}(K)}{\rho}\right)^p$. Let $\tau = \sup_K\|\mathcal{D}f\|$. According to the mean value theorem, $M_{0,\rho}\subset\mathcal{B}\big(f(\boldsymbol{x}),(\tau+2)\rho\big)$ and

$$\mathscr{L}_q(M_\rho) \leqslant \sum_{\boldsymbol{x}\in\Lambda_\rho}\mathscr{L}_q\Big(\mathcal{B}\big(f(\boldsymbol{x}),(\tau+2)\rho\big)\Big) \leqslant \frac{\sqrt{\pi}^p\,(\tau+2)^p}{\Gamma\left(\frac{p}{2}+1\right)} \times \big(\mathcal{D}\mathrm{iam}(K)\big)^p \times \rho^{q-p}\,.$$

Let $s\in\,]0,1[$. Then, from the Abel transformation,

$$\begin{aligned}\int_{\mathbb{R}^q\setminus f(K)} \log^+\frac{1}{d\big(\boldsymbol{y},f(K)\big)}\,\mathrm{d}\boldsymbol{y} &= \sum_{n=0}^{+\infty}\int_{M_{s^{n+1},s^n}} \log^+\frac{1}{d\big(\boldsymbol{y},f(K)\big)}\,\mathrm{d}\boldsymbol{y}\\ &\leqslant \sum_{n=0}^{+\infty}\log\frac{1}{s^{n+1}}\,\left[\mathscr{L}_q(M_{s^n})-\mathscr{L}_q(M_{s^{n+1}})\right]\\ &\leqslant -\log(s)\sum_{n=0}^{+\infty}\mathscr{L}_q(M_{s^n})\,.\end{aligned}$$

Hence the result as $s\in\,]0,1[$. ■

Lemma 3 *Assume* (H 1), (H 3), (H 4) *and*

(H′ 5) *Bounded regular variables implies bounded trajectories: For all individuals $i\in[\![1,n]\!]$, if there exists $b\in\mathbb{R}$ such that $\|(\boldsymbol{z}_{pop}^{reg},\boldsymbol{z}_i^{reg})\|_\infty < b$ then there exists $R\in\mathbb{R}_+^*$ such that $\|\vec{\boldsymbol{\gamma}}_i(\boldsymbol{z}_{pop},\boldsymbol{z}_i)\|_\infty < R$.*

Then, for any such ℓ,

$$\mathbb{E}_{P(\mathrm{d}\boldsymbol{y}^\ell)}\left[\sup_{\theta\in\Theta}\left(\sum_{i=1}^{\ell}\log q(\boldsymbol{y}_i|\theta)\right)^+\right] \;<\; +\infty\,.$$

Proof Let $i\in[\![1,\ell]\!]$, $\Gamma_i = \mathcal{I}m(\vec{\boldsymbol{\gamma}}_i)$ and $\Gamma^\ell = \prod_{i=1}^\ell\Gamma_i$. For all $\theta\in\Theta^\omega$,

$$\begin{aligned}q(\boldsymbol{y}_i|\theta) &= \frac{1}{(\sigma\sqrt{2\pi})^{k_i}}\int_{\overline{\mathcal{Z}}_i}\exp\left(-\frac{1}{2\sigma^2}\|\boldsymbol{y}_i-\vec{\boldsymbol{\gamma}}_i(\boldsymbol{z}_{\mathrm{pop}},\boldsymbol{z}_i)\|_2^2\right)q(\boldsymbol{z}_{\mathrm{pop}},\boldsymbol{z}_i|\theta)\;\mathrm{d}(\boldsymbol{z}_{\mathrm{pop}},\boldsymbol{z}_i)\\ &\leqslant \frac{1}{(\sigma\sqrt{2\pi})^{k_i}}\exp\left(-\frac{1}{2\sigma^2}d(\boldsymbol{y}_i,\Gamma_i)^2\right)\,.\end{aligned}$$

where d denotes the Euclidean distance on $\mathbb{R}^{k_i}$. Thus for all $\theta\in\Theta^\omega$,

$$\sum_{i=1}^{\ell}\log q(\boldsymbol{y}_i|\theta) \leqslant -\frac{k^\ell}{2}\log(2\pi\sigma^2) - \frac{1}{2\sigma^2}d(\boldsymbol{y}^\ell,\Gamma^\ell)^2$$

where d denotes now the Euclidean distance on $\mathbb{R}^{k^\ell}$, $k^\ell = \sum_{i=1}^{\ell} k_i$. As the right hand side is maximized for $\sigma^2 = \frac{1}{k^\ell} d(\boldsymbol{y}^\ell, \Gamma^\ell)^2$, there exists a constant $\lambda \in \mathbb{R}_+^*$ such that

$$\sup_{\theta\in\Theta} \left(\sum_{i=1}^{\ell} \log q(\boldsymbol{y}_i|\theta) \right)^+ \leqslant \lambda + k^\ell \log^+ \frac{1}{d(\boldsymbol{y}^\ell, \Gamma^\ell)} \,.$$

1. Assume there exists $i_0 \in [\![1, n]\!]$ such that that for all $b \in \mathbb{R}$, $\|(\boldsymbol{z}_{\text{pop}}^{\text{reg}}, \boldsymbol{z}_{i_0}^{\text{reg}})\|_\infty \geqslant b$.

   For all $r_1, r_2 \in \mathbb{R}$ we define a compact subset $\Gamma^\ell_{r_1,r_2}$ of Γ^ℓ by setting

   $$\bar{\mathcal{A}}(r_1, r_2) = \{\boldsymbol{z}^\ell \in \mathbb{R}^{p^\ell} \mid r_1 \leqslant \left\|(\boldsymbol{z}_{\text{pop}}^{\text{reg}}, \boldsymbol{z}_i^{\text{reg}})_{i\in[\![1,\ell]\!]}\right\|_\infty, \left\|(\boldsymbol{z}_{\text{pop}}^{\text{crit}}, \boldsymbol{z}_i^{\text{crit}})_{i\in[\![1,\ell]\!]}\right\|_\infty \leqslant r_2\}$$
   $$\text{and} \quad \Gamma^\ell_{r_1,r_2} = \{\vec{\boldsymbol{\gamma}}^\ell(\boldsymbol{z}^\ell) \mid \boldsymbol{z}^\ell \in \bar{\mathcal{A}}(r_1, r_2)\} \,.$$

   Especially, $\lim_{r_2\to\infty} \Gamma^\ell_{0,r_2} = \Gamma^\ell$. Moreover, $\vec{\boldsymbol{\gamma}}^\ell$ is differentiable *a.e.*, at least one-side differentiable everywhere and there exists $\tau \in \mathbb{R}$ such that $\sup_{\mathbb{R}^{p\ell}} \|\mathcal{D}_{\boldsymbol{z}^\ell} \vec{\boldsymbol{\gamma}}^\ell\| < \tau$. So, according to Lemma 2, for all $r_1, r_2 \in \mathbb{R}$, there exists $\mu \in \mathbb{R}$ which depends only on p^ℓ and k^ℓ such that $\mathbb{E}\left[\log^+ \frac{1}{d(\boldsymbol{y}^\ell, \Gamma^\ell_{r_1,r_2})}\right] < \mu\,(\tau+2)^{k^\ell}\; {r_2}^{p^\ell}$. As in the proof of Lemma 2, we set $\overline{\Gamma^\ell_{r_1,r_2}} = \{\boldsymbol{y}^\ell \in \mathbb{R}^{k^\ell} \mid d(\boldsymbol{y}^\ell, \Gamma^\ell_{r_1,r_2}) \leqslant 1\}$ and we have for all $r_1, r_2 \in \mathbb{R}$,

   $$\int_{\mathbb{R}^{k^\ell}} \log^+ \frac{1}{d(\boldsymbol{y}^\ell, \Gamma^\ell_{r_1,r_2})} P(\mathrm{d}\boldsymbol{y}^\ell) = \int_{\overline{\Gamma^\ell_{r_1,r_2}}} \log^+ \frac{1}{d(\boldsymbol{y}^\ell, \Gamma^\ell_{r_1,r_2})} P(\mathrm{d}\boldsymbol{y}^\ell) \leqslant \bar{\mu}\, {r_2}^{p^\ell} \sup_{\overline{\Gamma^\ell_{r_1,r_2}}} P(\boldsymbol{y}^\ell)$$

   where $\bar{\mu} = \mu\,(\tau+2)^{k^\ell} \in \mathbb{R}$. Let $R_1, R_2 \in \mathbb{N}$ such that $K \subset \bar{\mathcal{B}}(0, R_1)$ and $R_1 < R_2$. By definition of the distance to a subset, it comes that

   $$\mathbb{E}_{P(\mathrm{d}\boldsymbol{y}^\ell)}\left[\log^+ \frac{1}{d(\boldsymbol{y}^\ell, \Gamma^\ell_{0,R_2})}\right] \;\leqslant\; \bar{\mu}\, {R_1}^{p^\ell} \sup_{\overline{\Gamma^\ell_{0,R_1}}} P(\boldsymbol{y}^\ell) \;+\; \bar{\mu} \sum_{r=R_1}^{R_2-1} (r+1)^{p^\ell} \sup_{\overline{\Gamma^\ell_{r,r+1}}} P(\boldsymbol{y}^\ell) \,.$$

   The first term is finite as $P(\mathrm{d}\boldsymbol{y})$ is continuous. Besides, if $\boldsymbol{y}^\ell \in \overline{\Gamma^\ell_{r,r+1}}$, there exists $\boldsymbol{z}^\ell \in \bar{\mathcal{A}}(r, r+1)$ such that $\|\vec{\boldsymbol{\gamma}}^\ell(\boldsymbol{z}^\ell) - \boldsymbol{y}^\ell\|_\infty \leqslant 1$. Let $i \in [\![1, n]\!]$ and $v \in [\![1, p_{\text{pop}}^{\text{reg}} + p_{\text{ind}}^{\text{reg}}]\!]$ so that $\|(\boldsymbol{z}_{\text{pop}}^{\text{reg}}, \boldsymbol{z}_i^{\text{reg}})_{i\in[\![1,n]\!]}\|_\infty = |(\boldsymbol{z}_{\text{pop}}^{\text{reg}}, \boldsymbol{z}_i^{\text{reg}})_v|$. Such a couple exists due to the existence of i_0. Moreover, there exists $a_{i,v}\big((\boldsymbol{z}_{\text{pop}}^{\text{reg}}, \boldsymbol{z}_i^{\text{reg}})_{-v}\big)$ and $b_{i,v}\big((\boldsymbol{z}_{\text{pop}}^{\text{reg}}, \boldsymbol{z}_i^{\text{reg}})_{-v}\big)$ as in (H 4) and by definition of $\boldsymbol{z}^\ell$ and the infinite norm,

   $$\begin{aligned} \|\boldsymbol{y}^\ell\|_\infty \;\geqslant\; \|\vec{\boldsymbol{\gamma}}^\ell(\boldsymbol{z}^\ell)\|_\infty - 1 &\geqslant\; \|\vec{\boldsymbol{\gamma}}_i(\boldsymbol{z}_{\text{pop}}, \boldsymbol{z}_i)\|_\infty - 1 \\ &\geqslant\; a_{i,v}\,|(\boldsymbol{z}_{\text{pop}}^{\text{reg}}, \boldsymbol{z}_i^{\text{reg}})_v| \;+\; b_{i,v} - 1 \;\geqslant\; a_{i,v} \times r \;+\; b_{i,v} - 1 \,. \end{aligned}$$

   Consequently, $\sup_{\overline{\Gamma^\ell_{r,r+1}}} P(\boldsymbol{y}^\ell) \leqslant \sup\{P(\boldsymbol{y}^\ell) \mid \|\boldsymbol{y}^\ell\|_\infty \geqslant a_{i,v} \times r \;+\; b_{i,v} - 1\}$ and the series $\sum (r+1)^{p^\ell} \sup_{\overline{\Gamma^\ell_{r,r+1}}} P(\boldsymbol{y}^\ell)$ converge since $P(\mathrm{d}\boldsymbol{y})$ has a polynomial decay tail of degree bigger than $p^\ell + 1$ apart from K by assumption (H 3).

2. Assume that there exists $b \in \mathbb{R}$ such that for all $i \in [\![1, n]\!]$, $\|(\boldsymbol{z}_{\text{pop}}^{\text{reg}}, \boldsymbol{z}_i^{\text{reg}})\|_\infty \leqslant b$. Then, by assumption (H′ 5), there exists $R \in \mathbb{R}_+^*$ such that for all i, $\|\vec{\boldsymbol{\gamma}}_i(\boldsymbol{z}_{\text{pop}}, \boldsymbol{z}_i)\|_\infty < R$. In particular, $\|\vec{\boldsymbol{\gamma}}^\ell(\boldsymbol{z}^\ell)\|_\infty < R$ and $\Gamma^\ell \subset \bar{\mathcal{B}}(0, R)$. Thus,

$$\mathbb{E}_{P(\mathrm{d}\boldsymbol{y}^\ell)}\left[\log^+ \frac{1}{d(\boldsymbol{y}^\ell, \Gamma^\ell)}\right] \;\leqslant\; \mathbb{E}_{P(\mathrm{d}\boldsymbol{y}^\ell)}\left[\log^+ \frac{1}{d\big(\boldsymbol{y}^\ell, \bar{\mathcal{B}}(0,R)\big)}\right].$$

Yet, by still denoting $\overline{\bar{\mathcal{B}}(0,R)} = \{\boldsymbol{y}^\ell \in \mathbb{R}^{k^\ell} \mid d\big(\boldsymbol{y}^\ell, \bar{\mathcal{B}}(0,R)\big) \leqslant 1\}$ and applying Lemma 2 to the compact $K = \bar{\mathcal{B}}(0,R)$ and $f = Id$, there exists $\mu \in \mathbb{R}$ such that

$$\begin{aligned}\mathbb{E}_{P(\mathrm{d}\boldsymbol{y}^\ell)}\left[\log^+ \frac{1}{d\big(\boldsymbol{y}^\ell, \bar{\mathcal{B}}(0,R)\big)}\right] &= \int_{\overline{\bar{\mathcal{B}}(0,R)}} \log^+ \frac{1}{d\big(\boldsymbol{y}^\ell, \bar{\mathcal{B}}(0,R)\big)} P(\mathrm{d}\boldsymbol{y}^\ell) \\ &\leqslant\; \mu\, 3^{k^\ell}\, R^{p^\ell} \sup_{\overline{\bar{\mathcal{B}}(0,R)}} P(\boldsymbol{y}^\ell) \;< +\infty\,.\end{aligned}$$

Finally, in both cases, $\mathbb{E}_{P(\mathrm{d}\boldsymbol{y}^\ell)}\left[\sup_{\theta\in\Theta}\left(\sum_{i=1}^\ell \log q(\boldsymbol{y}_i|\theta)\right)^+\right] < +\infty$. ■

Lemma 4 *Assume* (H 1), (H 3), (H 4) *and* (H 5). *Let* $\overline{\mathscr{S}_{p_{ind}}^+(\mathbb{R})} = \mathscr{S}_{p_{ind}}^+(\mathbb{R}) \cup \{\infty\}$ *be the one point Alexandrov compactification of* $\mathscr{S}_{p_{ind}}^+(\mathbb{R})$ *and consider the compactification of the parameter space* Θ^ω

$$\overline{\Theta^\omega} = \left\{\theta = (\overline{\boldsymbol{z}_{pop}}, \Sigma, \sigma) \in \mathbb{R}^{p_{pop}} \times \overline{\mathscr{S}_{p_{ind}}^+(\mathbb{R})} \times \overline{\mathbb{R}^+} \mid \|\overline{\boldsymbol{z}_{pop}}\| \leqslant \omega\right\}$$

where $\overline{R^+} = [0, +\infty[\cup \{+\infty\}$. *Then, we have for all* $\omega \in \mathbb{R}$,

(C 1) $P(\mathrm{d}\boldsymbol{y}^\ell)$ *almost surely, for any sequence* $\theta_\kappa = \left(\overline{\boldsymbol{z}_{pop}}_\kappa, \Sigma_\kappa, \sigma_\kappa\right)$ *of elements from* Θ^ω *such that* $\lim_{\kappa\to\infty} \theta_\kappa \in \overline{\Theta^\omega} \setminus \Theta^\omega$,

$$\lim_{\kappa\to\infty} \sum_{i=1}^\ell \log q\left(\boldsymbol{y}_i|\theta_\kappa\right) = -\infty\,;$$

(C 2) *For any sequence* $(\theta_\kappa) \in \Theta^{\omega\mathbb{N}}$ *such that* $\lim_{\kappa\to\infty} \theta_\kappa \in \overline{\Theta^\omega} \setminus \Theta^\omega$,

$$\lim_{\kappa\to\infty} \mathbb{E}_{P(\mathrm{d}\boldsymbol{y}^\ell)}\left[\log q(y|\theta_\kappa)\right] = -\infty\,;$$

(C 3) *The mapping* $\theta \mapsto \mathbb{E}_{P(\mathrm{d}\boldsymbol{y}^\ell)}\left[\log q(y|\theta)\right]$ *is continuous on* Θ^ω *and* $\Theta_*^\omega \neq \varnothing$.

Proof We recall that a sequence $(\Sigma_\kappa)_{\kappa\in\mathbb{N}}$ of $\overline{\mathscr{S}_{p_{\text{ind}}}^+(\mathbb{R})}$ converge toward the point ∞ if it eventually steps out of every compact subset of $\mathscr{S}_{p_{\text{ind}}}^+(\mathbb{R})$. Let prove the three points in order.

1. As $\overline{\Theta^\omega}\backslash\Theta^\omega = \Big\{(\Sigma,\sigma) \in \overline{\mathscr{S}^+_{p_{\text{ind}}}(\mathbb{R})} \times \overline{\mathbb{R}^+} \;\Big|\; \|\Sigma\| = +\infty \wedge \|\Sigma^{-1}\| = +\infty \wedge \sigma \in \{0,+\infty\}\Big\}$, we proceed by disjunction. Let, for all $\kappa \in \mathbb{N}$, $\theta_\kappa = (\overline{\boldsymbol{z}_{pop}}_\kappa, \Sigma_\kappa, \sigma_\kappa) \in \Theta^\omega$.

   (i) Assume that, up to extraction of a subsequence, $\|\Sigma_\kappa\| \to \infty$ or $\|\Sigma_\kappa^{-1}\| \to \infty$.

   Let $M = \|\boldsymbol{y}^\ell\|_\infty$. For all individuals $i \in [\![1,n]\!]$ and all $\kappa \in \mathbb{N}$, the marginal density of $\boldsymbol{y}_i$ given θ_κ is given by :

$$q(\boldsymbol{y}_i|\theta_\kappa) = \frac{1}{(\sigma_\kappa\sqrt{2\pi})^{k_i}} \int_{\mathcal{Z}_{\text{pop}}\times\mathcal{Z}_i} \exp\left(-\frac{1}{2\sigma_\kappa^2}\|\boldsymbol{y}_i - \vec{\boldsymbol{\gamma}}_i(\boldsymbol{z}_{\text{pop}},\boldsymbol{z}_i)\|_2^2\right) q(\boldsymbol{z}_{\text{pop}},\boldsymbol{z}_i|\theta_\kappa)\ \mathrm{d}(\boldsymbol{z}_{\text{pop}},\boldsymbol{z}_i)\,.$$

   Let $x \geqslant 1$, $\mathcal{Z}^{\text{reg}}_{i,-1} = \Big\{\big(\boldsymbol{z}^{\text{reg}}_{i,2},\dots,\boldsymbol{z}^{\text{reg}}_{i,p^{\text{reg}}_{\text{ind}}}\big) \mid \boldsymbol{z}^{\text{reg}}_i \in \mathcal{Z}^{\text{reg}}_i\Big\}$ and likewise $\mathcal{Z}^{\text{reg}}_{\text{pop},-1}$. Let $\bar{\mathcal{B}}^x_{i,1}$ be the closed ball defined by

$$\bar{\mathcal{B}}^x_{i,1} = \bar{\mathcal{B}}^x_{i,1}\Big((\boldsymbol{z}^{\text{reg}}_{\text{pop}},\boldsymbol{z}^{\text{reg}}_i)_{-1}\Big) = \bar{\mathcal{B}}\left(0\,,\ \frac{xM - b_{i,1}\big((\boldsymbol{z}^{\text{reg}}_{\text{pop}},\boldsymbol{z}^{\text{reg}}_i)_{-1}\big)}{a_{i,1}\big((\boldsymbol{z}^{\text{reg}}_{\text{pop}},\boldsymbol{z}^{\text{reg}}_i)_{-1}\big)}\right)$$

   where $a_{i,1}\big((\boldsymbol{z}^{\text{reg}}_{\text{pop}},\boldsymbol{z}^{\text{reg}}_i)_{-1}\big)$ and $b_{i,1}\big((\boldsymbol{z}^{\text{reg}}_{\text{pop}},\boldsymbol{z}^{\text{reg}}_i)_{-1}\big)$ are defined as in (H 4). Thus, by slicing the integral in half and bounding the exponential on $\bar{\mathcal{B}}^x_{i,1}$ by 1,

$$\begin{aligned} q(\boldsymbol{y}_i|\theta_\kappa) \leqslant\ & \frac{1}{(\sigma_\kappa\sqrt{2\pi})^{k_i}} \int_{\bar{\mathcal{B}}^x_{i,1}\times\mathcal{Z}_{i,-1}} q(\boldsymbol{z}_{\text{pop}},\boldsymbol{z}_i|\theta_\kappa)\ \mathrm{d}(\boldsymbol{z}_{\text{pop}},\boldsymbol{z}_i) \\ & + \frac{1}{(\sigma_\kappa\sqrt{2\pi})^{k_i}} \int_{\bar{\mathcal{B}}^{x\,\complement}_{i,1}\times\mathcal{Z}_{i,-1}} \exp\left(-\frac{1}{2\sigma_\kappa^2}\|\boldsymbol{y}_i - \vec{\boldsymbol{\gamma}}_i(\boldsymbol{z}_{\text{pop}},\boldsymbol{z}_i)\|_2^2\right) \\ & \qquad q(\boldsymbol{z}_{\text{pop}},\boldsymbol{z}_i|\theta_\kappa)\ \mathrm{d}(\boldsymbol{z}_{\text{pop}},\boldsymbol{z}_i)\,. \end{aligned}$$

   where $\mathcal{Z}_{i,-1} = \mathcal{Z}^{\text{reg}}_{\text{pop},-1} \times \mathcal{Z}^{\text{crit}}_{\text{pop}} \times \mathcal{Z}^{\text{reg}}_{i,-1} \times \mathcal{Z}^{\text{crit}}_i$. Moreover, by conditioning,

$$\int_{\bar{\mathcal{B}}^x_{i,1}\times\mathcal{Z}_{i,-1}} q(\boldsymbol{z}_{\text{pop}},\boldsymbol{z}_i|\theta_\kappa)\ \mathrm{d}(\boldsymbol{z}_{\text{pop}},\boldsymbol{z}_i) = \int_{\bar{\mathcal{B}}^x_{i,1}} q(\boldsymbol{z}^{\text{reg}}_{\text{pop},1},\boldsymbol{z}^{\text{reg}}_{i,1}|\theta_\kappa)\ \mathrm{d}(\boldsymbol{z}^{\text{reg}}_{\text{pop},1},\boldsymbol{z}^{\text{reg}}_{i,1})\,.$$

   By continuity of $(\boldsymbol{z}^{\text{reg}}_{\text{pop},1},\boldsymbol{z}^{\text{reg}}_{i,1}) \mapsto q(\boldsymbol{z}^{\text{reg}}_{\text{pop},1},\boldsymbol{z}^{\text{reg}}_{i,1}|\theta_\kappa)$ and compactness of $\bar{\mathcal{B}}^x_{i,1}$,

$$\int_{\bar{\mathcal{B}}^x_{i,1}\times\mathcal{Z}_{i,-1}} q(\boldsymbol{z}_{\text{pop}},\boldsymbol{z}_i|\theta_\kappa)\ \mathrm{d}(\boldsymbol{z}_{\text{pop}},\boldsymbol{z}_i) \ \leqslant\ \sup_{\bar{\mathcal{B}}^x_{i,1}} q(\boldsymbol{z}^{\text{reg}}_{\text{pop},1},\boldsymbol{z}^{\text{reg}}_{i,1}|\theta_\kappa)\,\mathscr{L}_1(\bar{\mathcal{B}}^x_{i,1})\,.$$

   Since the marginal of a multivariate distribution is a multivariate distribution whose mean vector and covariance matrix are obtained by dropping the irrelevant variables, $\lim_{\|\Sigma_\kappa\|\to\infty} q(\boldsymbol{z}^{\text{reg}}_{\text{pop},1},\boldsymbol{z}^{\text{reg}}_{i,1}|\theta_\kappa) = 0$ and the first integral goes to zero as $\|\Sigma_\kappa\| \to \infty$.

   In the same way of the proof of Theorem 1, the marginal density $q(\boldsymbol{z}^{\text{reg}}_{\text{pop},1},\boldsymbol{z}^{\text{reg}}_{i,1}|\theta_\kappa)$ is controlled by the operator norm of the covariance matrix Σ_κ^{-1} from which we have drop the irrelevant variables. Hence, as $\|\Sigma_\kappa^{-1}\| \to \infty$, the first integral converges toward zero as well.

The second integral is maximized at $\sigma_\kappa^2 = \frac{1}{k_i}\|\boldsymbol{y}_i - \vec{\boldsymbol{\gamma}}_i(\boldsymbol{z}_{\text{pop}}, \boldsymbol{z}_i)\|^2$. Thus, due to the Cauchy-Schwarz inequality, there exists a constant $c \in \mathbb{R}_+^*$ such that for all $(\boldsymbol{z}_{\text{pop}}, \boldsymbol{z}_i) \in \bar{\mathcal{B}}_{i,1}^{x\,\complement} \times \mathcal{Z}_{i,-1}$,

$$\|\boldsymbol{y}_i - \vec{\boldsymbol{\gamma}}_i(\boldsymbol{z}_{\text{pop}}, \boldsymbol{z}_i)\|_2^2 \geqslant c\left(a_{i,1} \times \frac{xM - b_{i,1}}{a_{i,1}} + b_{i,1} - \|\boldsymbol{y}_i\|_\infty\right)^2 \geqslant c\left((x-1)M\right)^2$$

and by bounding the marginal density $q(\boldsymbol{z}_{\text{pop}}, \boldsymbol{z}_i|\theta_\kappa)$ on $\bar{\mathcal{B}}_{i,1}^{x\,\complement} \times \mathcal{Z}_{i,-1}$ by 1, the second integral is bounded from above by $\left(\frac{k_i}{2\pi}\right)^{\frac{k_i}{2}} \mathrm{e}^{-\frac{k_i}{2}} \frac{1}{\left(\sqrt{c}\,(x-1)M\right)^{k_i}}$. Therefore,

$$\limsup_{\kappa\to\infty} \sum_{i=1}^{\ell} \log q(\boldsymbol{y}_i|\theta_\kappa) \;\leqslant\; -\frac{k^\ell}{2}\Big[1 + \log(2\pi) + \log\left(\sqrt{c}\,(x-1)M\right)\Big] + \frac{1}{2}\sum_{i=1}^{\ell} k_i \log k_i\,.$$

Since x can be chosen arbitrarily large, we obtain the result for the case $\|\Sigma_\kappa\| \to +\infty$ as well as $\|\Sigma_\kappa^{-1}\| \to +\infty$.

(ii) Assume that, up to extraction of a subsequence, $\sigma_\kappa \to 0$ or $\sigma_\kappa \to \infty$.
Let $M = \|\boldsymbol{y}^\ell\|_\infty$. With the same notations as in the proof of Lemma 3, for all $\kappa \in \mathbb{N}$,

$$\sum_{i=1}^{\ell} \log q(\boldsymbol{y}_i|\theta_\kappa) \leqslant -\frac{k^\ell}{2}\log(2\pi\sigma_\kappa^2) - \frac{1}{2\sigma^2} d(\boldsymbol{y}^\ell, \Gamma^\ell)^2 \quad \text{where} \quad \Gamma^\ell = \mathcal{I}m(\vec{\boldsymbol{\gamma}}^\ell)$$

and d denotes the Euclidean distance on $\mathbb{R}^{k^\ell}$. Let us prove that $d(\boldsymbol{y}^\ell, \Gamma^\ell) > 0$ *a.s.* : the result will go along whatever $\sigma_\kappa \to 0$ or $\sigma_\kappa \to +\infty$ with the previous inequality.
Let $\mathcal{Z}^\ell = \mathcal{Z}_{\text{pop}} \times \prod_{i=1}^{\ell} \mathcal{Z}_i$.
Due to (H 4), for all $i \in [\![1, n]\!]$, $\lim_{\|(\boldsymbol{z}_{\text{pop}}^{\text{reg}}, \boldsymbol{z}_i^{\text{reg}})\|_\infty \to \infty} \|\gamma_i(\boldsymbol{z}_{\text{pop}}, \boldsymbol{z}_i)\|_\infty = +\infty$, and so for all $\varepsilon \in \mathbb{R}_+^*$ non-negative, there exists $R \in \mathbb{R}$ such as for all $\boldsymbol{z}^\ell \in \mathcal{Z}^\ell$ satisfying $\|\boldsymbol{z}^\ell\| > R$, $\|\vec{\boldsymbol{\gamma}}^{\boldsymbol{\ell}}(\boldsymbol{z}^\ell)\| > M + \varepsilon$. In particular, by definition of M, $\|\boldsymbol{y}^\ell - \vec{\boldsymbol{\gamma}}^\ell(\boldsymbol{z}^\ell)\|_\infty > 0$ for $\|(\boldsymbol{z}_{\text{pop}}^{\text{reg}}, \boldsymbol{z}_i^{\text{reg}})_{i\in[\![1,\ell]\!]}\|_\infty$ sufficiently large.
On the other hand, if at least a critical variable blows up, then by (H 5) there exists a critical trajectory γ_i^{crit} such that $\lim_{\|(\boldsymbol{z}_{\text{pop}}^{\text{crit}}, \boldsymbol{z}_i^{\text{crit}})\|_\infty \to \infty} \|\vec{\boldsymbol{\gamma}}_i(\boldsymbol{z}_{\text{pop}}, \boldsymbol{z}_i)\|_\infty = \gamma_i^{\text{crit}}$ and as soon as this variable becomes sufficiently large, $\boldsymbol{y}_i \neq \gamma_i^{\text{crit}}$ *a.s.* Thus, for $\|(\boldsymbol{z}_{\text{pop}}^{\text{crit}}, \boldsymbol{z}_i^{\text{crit}})_{i\in[\![1,\ell]\!]}\|_\infty$ sufficiently large, $\|\boldsymbol{y}^\ell - \vec{\boldsymbol{\gamma}}^\ell(\boldsymbol{z}^\ell)\|_\infty > 0$ *a.s.*
In other words, there exists $R \in \mathbb{R}_+^*$ such that for all $\boldsymbol{z}^\ell \in \mathcal{Z}^\ell$, if $\|\boldsymbol{z}^\ell\|_\infty > R$, then $\|\boldsymbol{y}^\ell - \vec{\boldsymbol{\gamma}}^\ell(\boldsymbol{z}^\ell)\|_\infty > 0$ *a.s.* So, by contraposition, if there exists $\boldsymbol{z}^\ell \in \mathcal{Z}^\ell$ such that $\|\boldsymbol{y}^\ell - \vec{\boldsymbol{\gamma}}^\ell(\boldsymbol{z}^\ell)\|_\infty = 0$ (at least *a.s.*) then $\|\boldsymbol{z}^\ell\|_\infty \leqslant R$. Especially, $\{\boldsymbol{z}^\ell \in \mathcal{Z}^\ell \mid \boldsymbol{y}^\ell = \vec{\boldsymbol{\gamma}}^\ell(\boldsymbol{z}^\ell)$ *a.s.*$\} \subset \bar{\mathcal{B}}(0, R)$. Since (H 3) assumes that $P(\mathrm{d}\boldsymbol{y})$ has a continuous density and since $\vec{\boldsymbol{\gamma}}^\ell\left(\bar{\mathcal{B}}(0,R)\right)$ is a submanifold of dimension $p^\ell < k^\ell$, $P\left[\,\boldsymbol{z}^\ell \in \bar{\mathcal{B}}(0,R)\,\right] = 0$. Hence, $\mathscr{L}_{k^\ell}\left(\left\{\boldsymbol{y}^\ell \mid d(\boldsymbol{y}^\ell, \mathcal{I}m(\vec{\boldsymbol{\gamma}}^\ell)) = 0\right\}\right) = 0$.

2. Let $f_\kappa(\boldsymbol{y}^\ell) = \sum_{i=1}^{\ell} \log q(\boldsymbol{y}_i|\theta_\kappa)$. From (C 1), we deduce that, up to extraction, the negative part $\left(f_\kappa(\boldsymbol{y}^\ell)\right)^-$ is almost surely a non-decreasing and non-negative sequence

converging to $+\infty$. From the monotone convergence theorem we then have

$$\liminf_{\kappa\to+\infty} \mathbb{E}_{P(\mathrm{d}\boldsymbol{y}^\ell)}\left[\left(f_\kappa(\boldsymbol{y}^\ell)\right)^-\right] = +\infty \quad \text{and so} \quad \lim_{\kappa\to+\infty} \mathbb{E}_{P(\mathrm{d}\boldsymbol{y}^\ell)}\left[\left(f_\kappa(\boldsymbol{y}^\ell)\right)^-\right] = +\infty\,.$$

Concerning the positive part $\left(f_\kappa(\boldsymbol{y}^\ell)\right)^+$, using the dominated convergence theorem, Lemma 3 and the point (C 1), we get $\lim_{\kappa\to+\infty} \mathbb{E}_{P(\mathrm{d}\boldsymbol{y}^\ell)}\left[\left(f_\kappa(\boldsymbol{y}^\ell)\right)^+\right] = 0$. Actually, for all $i \in [\![1, n]\!]$ the application $(\boldsymbol{z}_{\text{pop}}^{\text{reg}}, \boldsymbol{z}_i^{\text{reg}}) \mapsto \gamma_i^{\text{crit}}$ is continuous by continuity of the function $\vec{\boldsymbol{\gamma}}_i$ and so (H′ 5) holds.

Finally, we have proved that $\lim_{\kappa\to+\infty} \mathbb{E}_{P(\mathrm{d}\boldsymbol{y}^\ell)}\left[\sum_{i=1}^\ell \log q(\boldsymbol{y}_i|\theta_\kappa)\right] = -\infty$ and (C 2) follows immediately.

3. The continuity statement is straightforward. If Θ_*^ω is empty, any maximizing sequence θ_κ of $\mathbb{E}_{P(\mathrm{d}\boldsymbol{y}^\ell)}\left[\log q(\boldsymbol{y}^\ell|\theta)\right]$ satisfies (up to extraction of a subsequence) $\theta_\kappa \in \Theta^\omega$, $\|\Sigma_\kappa\| \to +\infty$, $\|\Sigma_\kappa^{-1x}\| \to +\infty$, $\sigma_\kappa \to 0$ or $\sigma_\kappa \to +\infty$, which is on contradiction with conclusion (C 2).

■

A.2 Proof of the consistency theorem

We follow in the following proof the classical approach of van der Vaart (2000).

Proof As in Lemma 4, let $\overline{\Theta^\omega}$ denote the one point Alexandrov compactification of the parameter space Θ^ω. We have already proved [Lemma 4 (C 3)] that $\Theta_*^\omega \neq \varnothing$. To achieve the proof, let us first demonstrate that for all $\theta_\infty \in \overline{\Theta^\omega}$ such that $\delta\left(\theta_\infty, \Theta_*^\omega\right) \geqslant \varepsilon$ there exists an open set $\mathcal{U} \subset \Theta^\omega$ such that

$$\frac{1}{\ell}\,\mathbb{E}_{P(\mathrm{d}\boldsymbol{y}^\ell)}\left[\sup_{\theta\in\mathcal{U}\cap\Theta^\omega} \sum_{i=1}^\ell \log q(\boldsymbol{y}_i|\theta)\right] < \mathbb{E}^*(\omega)\,. \tag{0}$$

Let $\varepsilon \geqslant 0$, $(\mathcal{U}_h) \subset \Theta^{\omega\mathbb{N}}$ be a non-increasing sequence of open subsets of Θ^ω for which $\bigcap_{h\geqslant 0} \mathcal{U}_h = \{\theta_\infty\}$ and f_h be the function defined by $f_h(\boldsymbol{y}^\ell) = \frac{1}{\ell}\sup_{\theta\in\mathcal{U}_h} \sum_{i=1}^\ell \log q(\boldsymbol{y}_i|\theta)$.

1. If $\theta_\infty \in \Theta^\omega$, through the continuity of the map $\theta \mapsto \sum_{i=1}^\ell \log q(\boldsymbol{y}_i|\theta)$ and the definition of the sequence $(\mathcal{U}_h)$, $\lim_{h\to+\infty} f_h(\boldsymbol{y}^\ell) = \frac{1}{\ell}\sum_{i=1}^\ell \log q(\boldsymbol{y}_i|\theta_\infty)$. So, according to the monotone convergence theorem, Lemma 3 and since $\theta_\infty \notin \Theta_*^\omega$,

$$\lim_{h\to+\infty} \mathbb{E}_{P(\mathrm{d}\boldsymbol{y}^\ell)}\left[f_h(\boldsymbol{y}^\ell)\right] = \frac{1}{\ell}\sum_{i=1}^\ell \mathbb{E}_{P(\mathrm{d}\boldsymbol{y}^\ell)}\left[\log q(\boldsymbol{y}_i|\theta_\infty)\right] < \mathbb{E}^*(\omega)\,.$$

2. If $\theta_\infty \notin \Theta^\omega$, we can prove that for all observations $\boldsymbol{y}^\ell \in \mathbb{R}^{k^\ell}$ $\lim_{h\to\infty} f_h(\boldsymbol{y}^\ell) = -\infty$ $P(\mathrm{d}\boldsymbol{y}^\ell)$ *a.s.* We proceed by contradiction : assume that there exists a measurable set $A \in \mathscr{B}(\mathbb{R}^{k^\ell})$ such that $\mathbb{P}(\boldsymbol{y}^\ell \in A) > 0$ and for all $\boldsymbol{y}^\ell \in A$, $\inf_{h\in\mathbb{N}} f_h(\boldsymbol{y}^\ell) > -\infty$. Then,

by definition of the *infimum*, for all $\boldsymbol{y}^\ell \in A$ there exists a sequence $(h_n) \in \mathbb{R}^{\mathbb{N}}$ such as $\liminf_{n\to+\infty} f_{h_n}(y) > -\infty$. However for all $\boldsymbol{y}^\ell \in A$, $h \mapsto f_h(\boldsymbol{y}^\ell)$ is non-increasing and reaches its *infimum* limit for $h = +\infty$ and thus $\lim_{n\to+\infty} \mathcal{U}_{h_n} = \mathcal{U}_\infty = \{\theta_\infty\}$. Finally, up to considering a sequence $(\theta_{n,n'}) \in \mathcal{U}_{h_n}^{\mathbb{N}}$ for all subsets $\mathcal{U}_{h_n} \subset \Theta^\omega$ such that for all $n \in \mathbb{N}$, $\lim_{n'\to+\infty} \sum_{i=1}^{\ell} \log q(\boldsymbol{y}_i|\theta_{n,n'}) = \sup_{\theta\in\mathcal{U}_n} \sum_{i=1}^{\ell} \log q(\boldsymbol{y}_i \mid \theta)$, concatenating, reindexing those sequences and using the continuity of the map $\theta \mapsto \sum_{i=1}^{\ell} \log q(\boldsymbol{y}_i|\theta)$ we know that there exists a sequence $(\theta_n) \in \Theta^{\omega\mathbb{N}}$ such that

$$\lim_{n\to\infty} \theta_n = \theta_\infty \qquad \text{and} \qquad \liminf_{n\to+\infty} \sum_{i=1}^{\ell} \log q(\boldsymbol{y}_i|\theta_n) > -\infty\,.$$

Moreover, $\theta_\infty = \left(\overline{\boldsymbol{z}_{pop}}_\infty\,,\, \Sigma_\infty\,,\, \sigma_\infty\right) \in \overline{\Theta^\omega} \setminus \Theta^\omega$ and thus $\sigma_\infty \in \{0, +\infty\}$, $\|\Sigma_\infty\| = +\infty$ or $\|\Sigma_\infty^{-1}\| = +\infty$, in contradiction to [Lemma 4 (C 1)]. So for all observations $\boldsymbol{y}$, $\lim_{h\to\infty} f_h(\boldsymbol{y}^\ell) = -\infty$ $P(\mathrm{d}\boldsymbol{y})$ *a.s.* As in the proof of Lemma 4, Hypothesis (H 5) implies (H′ 5) and according to Lemma 3 and the monotone convergence theorem,

$$\lim_{h\to+\infty} \mathbb{E}_{P(\mathrm{d}\boldsymbol{y}^\ell)}\left[f_h(\boldsymbol{y}^\ell)\right] = -\infty < \mathbb{E}^*(\omega)\,.$$

That is, in both cases $\lim_{h\to+\infty} \mathbb{E}_{P(\mathrm{d}\boldsymbol{y}^\ell)}\left[f_h(\boldsymbol{y}^\ell)\right] < \mathbb{E}^*(\omega)$ and there exists an open set $\mathcal{U} \subset \Theta^\omega$ such that $\frac{1}{\ell}\,\mathbb{E}_{P(\mathrm{d}\boldsymbol{y}^\ell)}\left[\sup_{\theta\in\mathcal{U}\cap\Theta^\omega} \sum_{i=1}^{\ell} \log q(\boldsymbol{y}_i|\theta)\right] < \mathbb{E}^*(\omega)$ as announced.

Let $K_\varepsilon = \{\theta \in \overline{\Theta^\omega} \mid \delta(\theta, \Theta_*^\omega) \geqslant \varepsilon\}$. Through the compactness of K_ε, there exists an open finite cover $(\mathcal{U}_\alpha)_{\alpha\in[\![1,A]\!]}$ of K_ε satisfying (0). Thus, denoting $q_n = \lfloor \frac{n}{\ell} \rfloor$ and $r_n = n - q_n\ell$ the quotient and the rest of the euclidean division of n by ℓ , we get for all $\theta \in K_\varepsilon$,

$$\sup_{\theta\in K_\varepsilon\cap\Theta^\omega} \sum_{i=1}^{n} \log q(\boldsymbol{y}_i|\theta) \leqslant \sup_{\alpha\in[\![1,A]\!]} \left(\sum_{q=0}^{q_n} \sup_{\theta\in\mathcal{U}_\alpha\cap\Theta^\omega} \sum_{r=1}^{\ell} \log q(\boldsymbol{y}_{q\ell+r}|\theta) + \sup_{\theta\in\mathcal{U}_\alpha\cap\Theta^\omega} \sum_{r=\ell+1}^{r_n} \log q(\boldsymbol{y}_{q_n\ell+r}|\theta) \right).$$

However, according to the strong law of large numbers, Assumption (H 2) and (0),

$$\lim_{q_n\to\infty} \frac{1}{q_n} \sum_{q=0}^{q_n} \sup_{\theta\in\mathcal{U}_\alpha\cap\Theta^\omega} \sum_{r=1}^{\ell} \log q(\boldsymbol{y}_{q\ell+r}|\theta) \leqslant \ell\,\mathbb{E}^*(\omega)$$

hence, since $\lim_{n\to+\infty} q_n = +\infty$ and $r_n < \ell$ for all $n \in \mathbb{N}$,

$$\limsup_{n\to\infty} \left[\frac{q_n}{n} \sup_{\alpha\in[\![1,A]\!]} \left(\frac{1}{q_n} \sum_{q=0}^{q_n} \sup_{\theta\in\mathcal{U}_\alpha\cap\Theta^\omega} \sum_{r=1}^{\ell} \log q(\boldsymbol{y}_{q\ell+r}|\theta) \right) \right] = \frac{1}{\ell} \times \sup_{\alpha\in[\![1,A]\!]} \left(\mathbb{E}_{P(\mathrm{d}\boldsymbol{y}^\ell)} \left[\sup_{\theta\in\mathcal{U}_\alpha\cap\Theta^\omega} \sum_{r=1}^{\ell} \log q(\boldsymbol{y}_{q_n\ell+r}|\theta) \right] \right) < \mathbb{E}^*(\omega)\,.$$

Otherwise, for all $r \in [\![\ell+1, \ell_n]\!]$, $\log q(\boldsymbol{y}_{q_n\ell+r}|\theta) \leqslant -k^\ell \log q(\sigma\sqrt{2\pi})$ so

$$\frac{1}{n} \sup_{\alpha\in[\![1,A]\!]} \left(\sup_{\theta\in\mathcal{U}_\alpha\cap\Theta^\omega} \sum_{r=\ell+1}^{r_n} \log q(\, \boldsymbol{y}_{q_n\ell+r}|\theta\,) \right) \leqslant \frac{k^\ell(r_n-1)}{n} \log(\sigma\sqrt{2\pi})\,.$$

Thereafter $\limsup_{n\to\infty} \left[\frac{1}{n} \sup_{\alpha\in[\![1,A]\!]} \left(\sup_{\theta\in\mathcal{U}_\alpha\cap\Theta^\omega} \sum_{r=\ell+1}^{r_n} \log q(\, \boldsymbol{y}_{q_n\ell+r}|\theta\,) \right) \right] \leqslant 0$ and

$$\limsup_{n\to\infty} \frac{1}{n} \sup_{\theta\in K_\varepsilon\cap\Theta^\omega} \sum_{i=1}^{n} \log q(\boldsymbol{y}_i|\theta) < \mathbb{E}^*(\omega)\,. \tag{1}$$

By definition of Θ_*^ω and according to the strong law of large numbers and (H 2), for all $\theta^* \in \Theta_*^\omega$ $\lim_{n\to\infty} \frac{1}{n}\sum_{i=1}^n \log q(\boldsymbol{y}_i|\theta^*) = \mathbb{E}^*(\omega)$ *a.s.* Moreover for all $i \in [\![1,n]\!]$,

$$q(\boldsymbol{y}_i|\hat{\theta}_n) = \frac{q(\hat{\theta}_n \mid \boldsymbol{y}_i)\, q(\boldsymbol{y}_i)}{q_{prior}(\hat{\theta}_n)} \;\geqslant\; \frac{q(\theta_* \mid \boldsymbol{y}_i)\, q(\boldsymbol{y}_i)}{q_{prior}(\hat{\theta}_n)} = \frac{q(\boldsymbol{y}_i|\theta_*)\, q_{prior}(\theta_*)}{q_{prior}(\hat{\theta}_n)}$$

and so $\sum_{i=1}^n \log q(\boldsymbol{y}_i|\hat{\theta}_n) \geqslant \sum_{i=1}^n \log q(\boldsymbol{y}_i|\theta_*) + \Big(\log q_{prior}(\theta_*) - \log q_{prior}(\hat{\theta}_n)\Big)$. Since q_{prior} is upper-bounded on Θ^ω, there exists $M \in \mathbb{R}^+$ such that

$$\frac{1}{n}\Big(\log q_{prior}(\theta_*) - \log q_{prior}(\hat{\theta}_n)\Big) \geqslant \frac{1}{n} \log\left(\frac{q_{prior}(\theta_*)}{M}\right)$$

i.e. $\liminf_{n\to+\infty} \frac{1}{n}\Big(\log q_{prior}(\theta_*) - \log q_{prior}(\hat{\theta}_n)\Big) \geqslant 0$ and

$$\liminf_{n\to+\infty} \frac{1}{n} \sum_{i=1}^{n} \log q(\boldsymbol{y}_i|\hat{\theta}_n) \geqslant \mathbb{E}^*(\omega)\,. \tag{2}$$

The result follows from Equations 1 and 2 by contradiction : Assume that for all $n \in \mathbb{N}$, $\hat{\theta}_n \in K_\varepsilon$ *i.e.* that $\delta(\hat{\theta}_n, \Theta_*^\omega) \geqslant \varepsilon$. Then $\sum_{i=1}^n \log q(\boldsymbol{y}_i|\hat{\theta}_n) \leqslant \sup_{\theta\in K_\varepsilon\cap\Theta^\omega} \sum_{i=1}^n \log q(\boldsymbol{y}_i|\theta)$ and by taking the limit superior, we get

$$\mathbb{E}^*(\omega) \overset{(2)}{\leqslant} \limsup_{n\to\infty} \frac{1}{n} \sum_{i=1}^{n} \log q(\boldsymbol{y}_i|\hat{\theta}_n) \overset{(1)}{<} \mathbb{E}^*(\omega)$$

i.e. $\mathbb{E}^*(\omega) < \mathbb{E}^*(\omega)$. Hence $\lim_{n\to\infty} \mathbb{P}\left[\delta(\hat{\theta}_n, \Theta_*^\omega) \geqslant \varepsilon\right] = 0$. ■

References

Stéphanie Allassonnière, Yali Amit, and Alain Trouvé. Toward a coherent statistical framework for dense deformable template estimation. *Journal of the Royal Statistical Society. Series B (Statistical Methodology)*, 69(1):3–29, 2007.

Stéphanie Allassonnière, Estelle Kuhn, and Alain Trouvé. Construction of Bayesian deformable models via a stochastic approximation algorithm: A convergence study. *Bernoulli*, 16(3):641–678, 2010.

Yves F. Atchadé. An adaptive version for the Metropolis adjusted Langevin algorithm with a truncated drift. *Methodology and Computing in Applied Probability*, 8(2):235–254, 2006.

Alexandre Bône, Olivier Colliot, and Stanley Durrleman. Learning distributions of shape trajectories from longitudinal datasets: A hierarchical model on a manifold of diffeomorphisms. In *Computer Vision and Pattern Recognition*, Salt Lake City, United States, 2018.

Juliette Chevallier, Stéphane Oudard, and Stéphanie Allassonnière. Learning spatiotemporal piecewise-geodesic trajectories from longitudinal manifold-valued data. In *Neural Information Processing Systems*, number 30 in Advances in Neural Information Processing Systems, Long Beach, CA, USA, 2017.

Bernard Delyon, Marc Lavielle, and Eric Moulines. Convergence of a stochastic approximation version of the EM algorithm. *The Annals of Statistics*, 27(1):94–128, 1999.

Arthur Dempster, Nan M. Laird, and Donald B. Rubin. Maximum likelihood from incomplete data via the EM algorithm. *Journal of the Royal Statistical Society. Series B (Statistical Methodology)*, 39(1):1–38, 1977.

Bernard Escudier, Camillo Porta, Mlanie Schmidinger, Nathalie Rioux-Leclercq, Axel Bex, Vincent S. Khoo, Viktor Gruenvald, and Alan Horwich. Renal cell carcinoma: ESMO clinical practice guidelines for diagnosis, treatment and follow-up. *Annals of Oncology*, 27(suppl 5):v58–v68, 2016.

Sylvestre Gallot, Dominique Hulin, and Jacques Lafontaine. *Riemannian Geometry*. Universitext. Springer-Verlag Berlin Heidelberg, 3 edition, 2004.

Christophe Giraud. *Introduction to High-Dimensional Statistics*. Chapman & Hall/CRC Monographs on Statistics & Applied Probability. Taylor & Francis, 2014.

Igor Koval, Jean-Baptiste Schiratti, Alexandre Routier, Michael Bacci, Olivier Colliot, Stephanie Allassonniere, and Stanley Durrleman. Spatiotemporal propagation of the cortical atrophy: Population and individual patterns. *Frontiers in Neurology*, 9, 2018.

Estelle Kuhn and Marc Lavielle. Maximum likelihood estimation in nonlinear mixed effects models. *Computational Statistics & Data Analysis*, 49(4):1020–1038, 2005.

Nan M. Laird and James H. Ware. Random-effects models for longitudinal data. *Biometrics*, 38(4):963–974, 1982.

Marc Lavielle. *Mixed Effects Models for the Population Approach: Models, Tasks, Methods and Tools*. CRC Biostatistics Series. Chapman and Hall, 2014.

Marc Lavielle and Leon Aarons. What do we mean by identifiability in mixed effects models? *Journal of Pharmacokinetics and Pharmacodynamics*, 43(1):111–122, February 2016.

J. Kevin Milliken and Steven D. Edland. Mixed effect models of longitudinal alzheimer's disease data: A cautionary note. *Statistics in Medicine*, 19(11-12):1617–1629, 2000.

B Ribba, NH Holford, P Magni, I Trocniz, I Gueorguieva, P Girard, C Sarr, M Elishmereni, C Kloft, and LE Friberg. A review of mixed-effects models of tumor growth and effects of anticancer drug treatment used in population analysis. *CPT: Pharmacometrics & Systems Pharmacology*, 3(5):1–10, 2014.

Christian P. Robert and George Casella. *Monte Carlo Statistical Methods*. Springer Texts in Statistics. Springer-Verlag New York, 1999.

Gareth O. Roberts and Jeffrey S. Rosenthal. Coupling and ergodicity of adaptive Markov chain Monte Carlo algorithms. *Journal of Applied Probability*, 44(2):458–475, 03 2007.

Gareth O. Roberts and Jeffrey S. Rosenthal. Examples of adaptive MCMC. *Journal of Computational and Graphical Statistics*, 18(2):349–367, 2009.

Jean-Baptiste Schiratti, Stéphanie Allassonnière, Olivier Colliot, and Stanley Durrleman. Learning spatiotemporal trajectories from manifold-valued longitudinal data. In *Neural Information Processing Systems*, number 28 in Advances in Neural Information Processing Systems, Montréal, Canada, 2015.

Jean-Baptiste Schiratti, Stéphanie Allassonnière, Olivier Colliot, and Stanley Durrleman. A Bayesian mixed-effects model to learn trajectories of changes from repeated manifold-valued observations. *Journal of Machine Learning Research*, 18(133):1–33, 2017.

Patrick Therasse, Susan G. Arbuck, Elizabeth A. Eisenhauer, Jantien Wanders, Richard S. Kaplan, Larry Rubinstein, Jaap Verweij, Martine Van Glabbeke, Allan T. van Oosterom, Michaele C. Christian, and Steve G. Gwyther. New guidelines to evaluate the response to treatment in solid tumors. *Journal of the National Cancer Institute*, 92(3):205–216, 2000.

Adrianus Willem van der Vaart. *Asymptotic Statistics*. Cambridge Series in Statistical and Probabilistic Mathematics. Cambridge University Press, 2000.